# 10th International Conference on Quarks and Nuclear Physics (QNP 2024)

July 11, 2024

# Compatibility between $e^+e^-$ and tau decay data in the di-pion channels and implications for $a_\mu$

Alejandro Miranda
IFAE, Spain

In collaboration with:
Gabriel Lopez Castro (Cinvestav, IPN, Mexico)
Pablo Roig (Cinvestav, IPN, Mexico)

IFAE
Institut de Física d'Altes Energies

BIST Barcelona Institute of Science and Technology

Generalitat de Catalunya
Departament de Recerca i Universitats

# Hadronic vacuum polarization

- At low energies **QCD** gets **strongly interacting** and a **perturbative calculation** is **not feasible**.
- Luckily, **analyticity** and **unitarity** allow us to express the **leading hadronic vacuum polarization** (**HVP**) contributions via a **dispersion relation** in terms of **experimental data**:

$$a_\mu^{\text{HVP,LO}} = \frac{\alpha^2}{3\pi^2} \int_{m_\pi^2}^{\infty} ds \frac{K(s)}{s} R(s),$$

Gourdin, De Rafael. Nucl.Phys.B 10 (1969) 667-674

where *K(s)* is a **Kernel function** ⟹ $K(s) \sim 1/s,$

$$R(s) = \frac{\sigma^0(e^+e^- \to \text{hadrons}(+\gamma))}{\sigma_{pt}}, \quad \sigma_{pt} = \frac{4\pi\alpha^2}{3s}$$

- An evaluation of the **HVP, LO** contribution can be obtained from the measurements of **$\sigma(e^+e^- \to$ hadrons)** or the **$\tau \to \nu_\tau$ + hadron** decays which can be related to the **isovector component** of the **$e^+e^- \to$ hadrons** cross section through **isospin-symmetry**.
- Since both are subject to **theoretical uncertainties**, it is a good strategy to keep using both.

# Hadronic vacuum polarization

- About 73% of the contributions to the HVP and 58% of the total uncertainty correspond to the $\pi^+\pi^-(\gamma)$ final state at low energies $(4m_\pi^2 \leq s \leq 0.8\,\mathrm{GeV}^2)$.
- For the two-pion final state,

$$\sigma_{\pi^+\pi^-}(s) = \frac{\pi\alpha^2\beta^3_{\pi^-\pi^+}(s)}{3s}\,|F_V(s)|^2\,,$$

- Including isospin-breaking corrections at LO, we have

$$\sigma_{\pi^+\pi^-}(s) = \left[\frac{K_\sigma(s)}{K_\Gamma(s)}\frac{d\Gamma_{\pi\pi[\gamma]}}{ds}\right]\frac{R_{IB}(s)}{S_{EW}},$$

where $R_{IB}(s) = \frac{FSR(s)}{G_{EM}(s)}\frac{\beta^3_{\pi^+\pi^-}}{\beta^3_{\pi^0\pi^-}}\left|\frac{F_V(s)}{f_+(s)}\right|^2,$

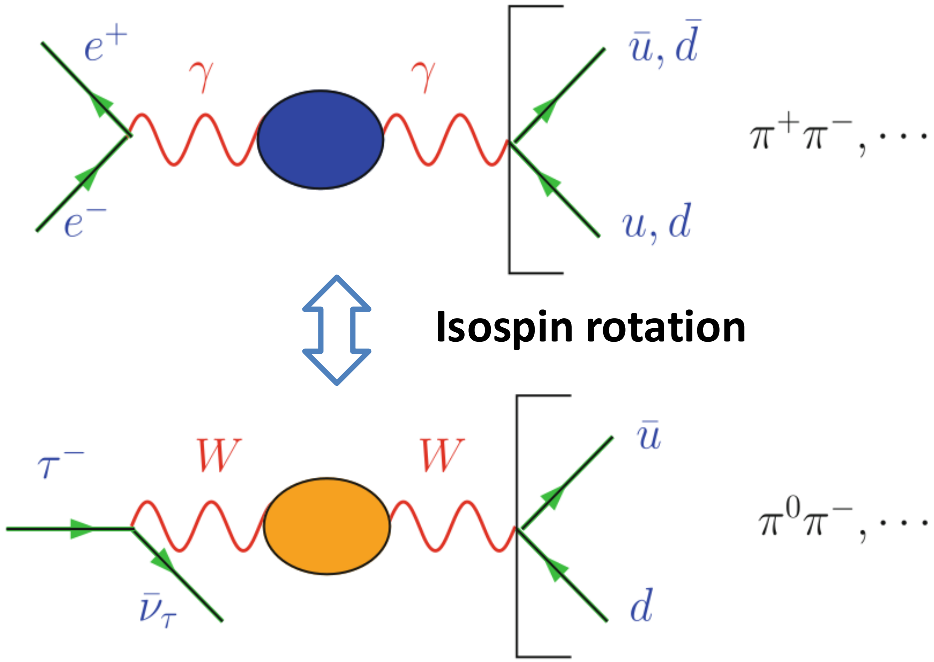


F. Jegerlehner. Springer Tracts Mod.Phys. 274 (2017)

- The ratio of neutral to charged current di-pion form factor and the long-distance em RadCor are challenging.
- $G_{EM}(s)$ receives contributions from real and virtual photons.

Cirigliano et al. Phy. Lett. B513 (2001). JHEP 08 (2002) 002

# Isospin-breaking corrections to $B_{\pi\pi 0}$

- Another important independent **cross-check** of the **IB corrections** is provided by the prediction of the **branching ratio** based on **CVC**.

$$\mathcal{B}^{\mathrm{CVC}}_{\pi\pi^0} = \mathcal{B}_e \int_{4m_\pi^2}^{m_\tau^2} ds\, \sigma_{\pi^+\pi^-(\gamma)}(s) \mathcal{N}(s) \frac{S_{\mathrm{EW}}}{R_{\mathrm{IB}}(s)}$$

The **IB corrections** to $\mathcal{B}^{\mathrm{CVC}}_{\pi\pi^0}$ can be evaluated from

$$\Delta\mathcal{B}^{\mathrm{CVC}}_{\pi\pi^0} = \mathcal{B}_e \int_{4m_\pi^2}^{m_\tau^2} ds\, \sigma_{\pi^+\pi^-(\gamma)}(s) \mathcal{N}(s) \left( \frac{S_{\mathrm{EW}}}{R_{\mathrm{IB}}(s)} - 1 \right)$$

$$R_{IB}(s) = \frac{FSR(s)}{G_{EM}(s)} \frac{\beta^3_{\pi^+\pi^-}}{\beta^3_{\pi^0\pi^-}} \left| \frac{F_V(s)}{f_+(s)} \right|^2,$$

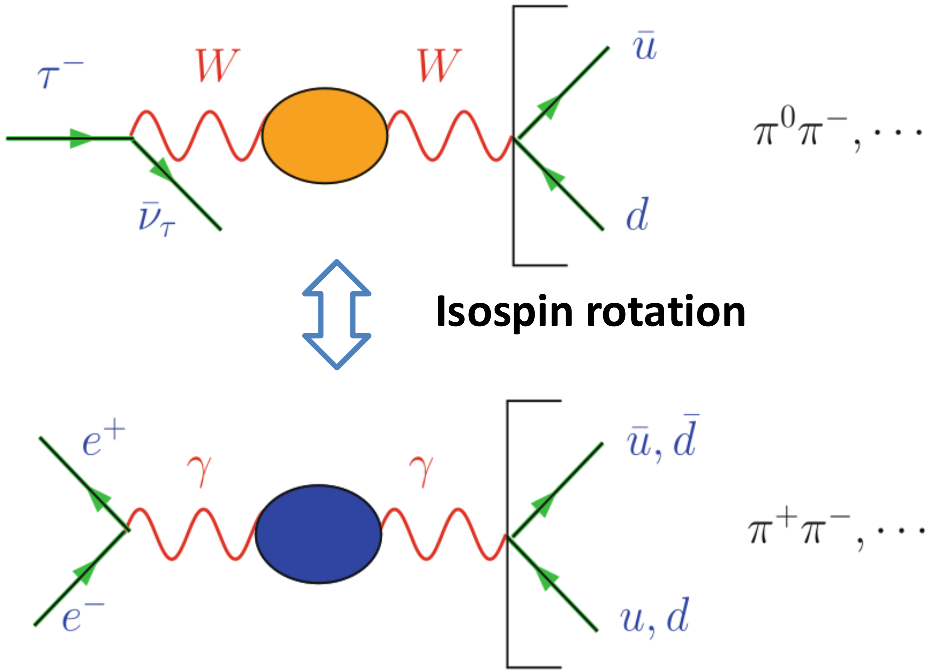


F. Jegerlehner. Springer Tracts Mod.Phys. 274 (2017)

# Isospin-breaking corrections

| Source | $\Delta\mathcal{B}^{\rm CVC}_{\pi^-\pi^0}$ $(10^{-2})$ GS model | KS model |
|---|---|---|
| $S_{\rm EW}$ | $+0.57 \pm 0.01$ | |
| $G_{\rm EM}$ | $-0.07 \pm 0.17$ | |
| FSR | $-0.19 \pm 0.02$ | |
| $\rho$–$\omega$ interference | $-0.01 \pm 0.01$ | $-0.02 \pm 0.01$ |
| $m_{\pi^\pm} - m_{\pi^0}$ effect on $\sigma$ | $+0.19$ | |
| $m_{\pi^\pm} - m_{\pi^0}$ effect on $\Gamma_\rho$ | $-0.22$ | |
| $m_{\rho^\pm} - m_{\rho^0_{\rm bare}}$ | $+0.08 \pm 0.08$ | $+0.09 \pm 0.08$ |
| $\pi\pi\gamma$, electrom. decays | $+0.34 \pm 0.03$ | $+0.37 \pm 0.04$ |
| Total | $+0.69 \pm 0.19$ | $+0.72 \pm 0.19$ |
| | $+0.69 \pm 0.22$ | |

Eur. Phys. J. C66, 127 (2010)

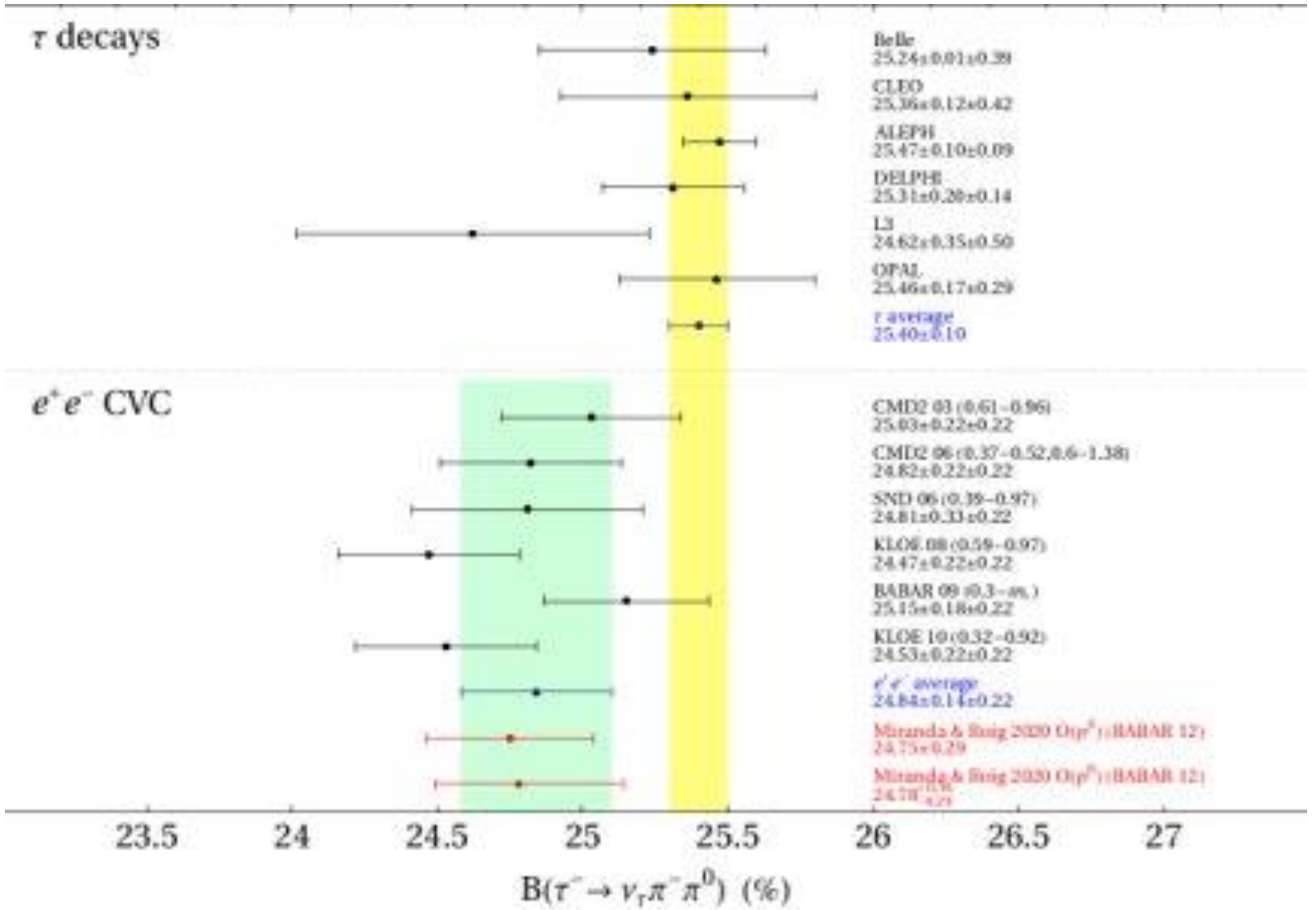


Phys. Rev. D 102 (2020) 114017

# Form factors

- Now let us analyze in more detail the **IB effects** in the **form factors**.
- These **IB breaking corrections** were studied by **Davier et al '09** using the **Gounaris-Sakurai** (GS) and **Kühn-Santamaria** (KS) parametrization.

$$R_{IB}(s) = \frac{FSR(s)}{G_{EM}(s)} \frac{\beta^3_{\pi^+\pi^-}}{\beta^3_{\pi^0\pi^-}} \left| \frac{F_V(s)}{f_+(s)} \right|^2,$$

$$F_\pi(s) = \frac{1}{1 + c_{\rho'} + c_{\rho''}} \left( BW^{GS}_\rho(s, m_\rho, \Gamma_\rho) \left(1 + \delta_{\rho\omega} \frac{s}{m^2} BW^{KS}_\omega(s, m_\omega, \Gamma_\omega)\right) + c_{\rho'} BW^{GS}_{\rho'}(s, m_{\rho'}, \Gamma_{\rho'}) + c_{\rho''} BW^{GS}_{\rho''}(s, m_{\rho''}, \Gamma_{\rho''}) \right),$$

$$BW^{GS}(s, m, \Gamma) = \frac{m^2 \left[1 + d(m)\Gamma/m\right]}{m^2 - s + f(s, m, \Gamma) - im\Gamma(s, m, \Gamma)}, \qquad BW^{KS}(s, m, \Gamma) = \frac{m^2}{m^2 - s - im\Gamma(s, m, \Gamma)}$$

- The **Guerrero-Pich** (GP) parametrization was employed by **Cirigliano et al '02** .

$$F_V(t) = \frac{m^2_{\rho^0}}{m^2_{\rho^0} - t - im_{\rho^0}\Gamma_{\rho^0}(t)} \left\{ \exp\left[2\tilde{H}_{\pi^+\pi^-}(t) + \tilde{H}_{K^+K^-}(t)\right] - \frac{\theta_{\rho\omega}}{3m^2_{\rho^0}} \frac{t}{m^2_\omega - t - i\, m_\omega \Gamma_\omega} \right\}$$

**Θρω is a real mixing parameter**

$$f_+(t) = \frac{m^2_{\rho^+}}{m^2_{\rho^+} - t - im_{\rho^+}\Gamma_{\rho^+}(t)} \exp\left\{2\tilde{H}_{\pi^+\pi^0}(t) + \tilde{H}_{K^+K^0}(t)\right\} + f^{\rm elm}_{\rm local} + \cdots ,$$

# IB corrections to FF

- **IB corrections** in the ratio of the form factors in the **GS model**.

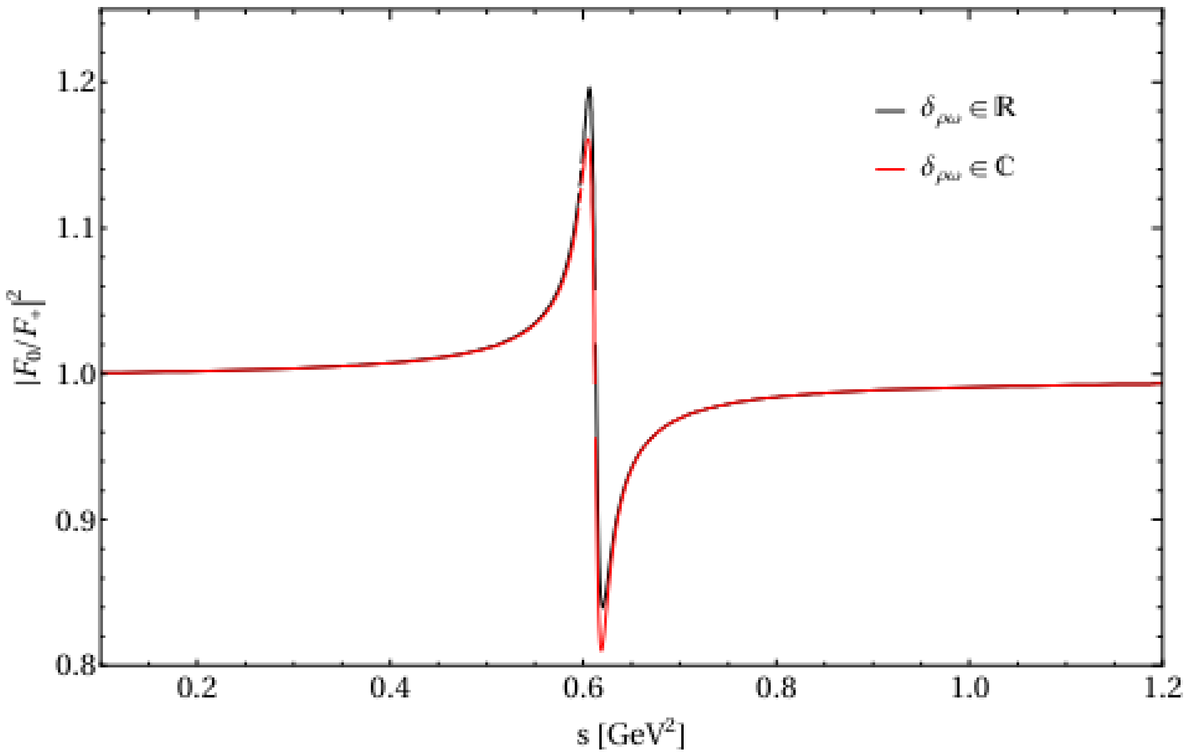


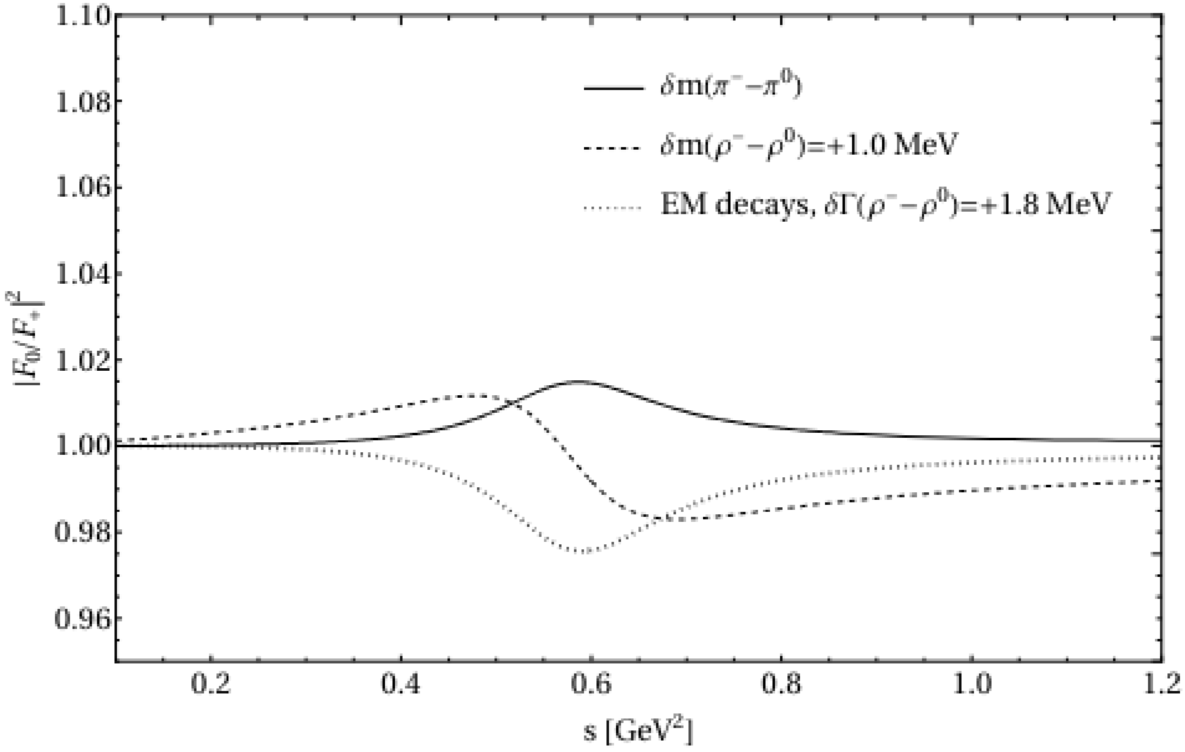

# IB corrections to FF

- **IB corrections** in the ratio of the form factors in the **GP model**.

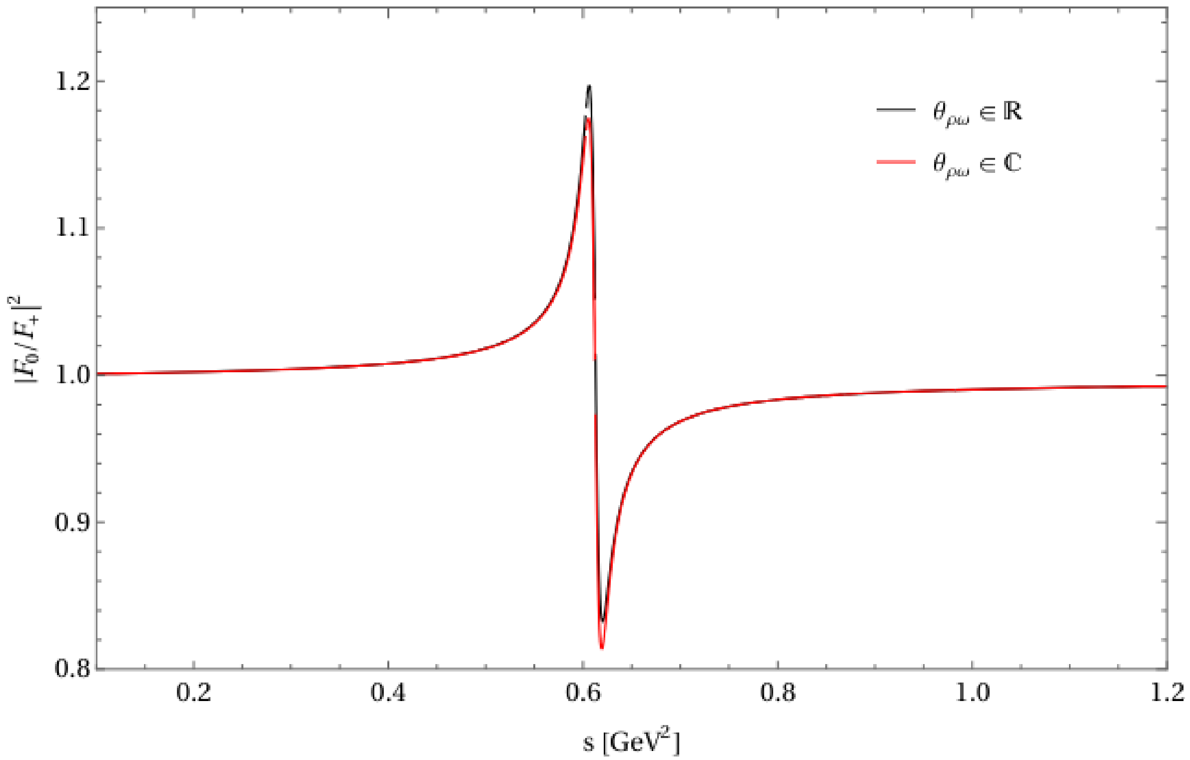


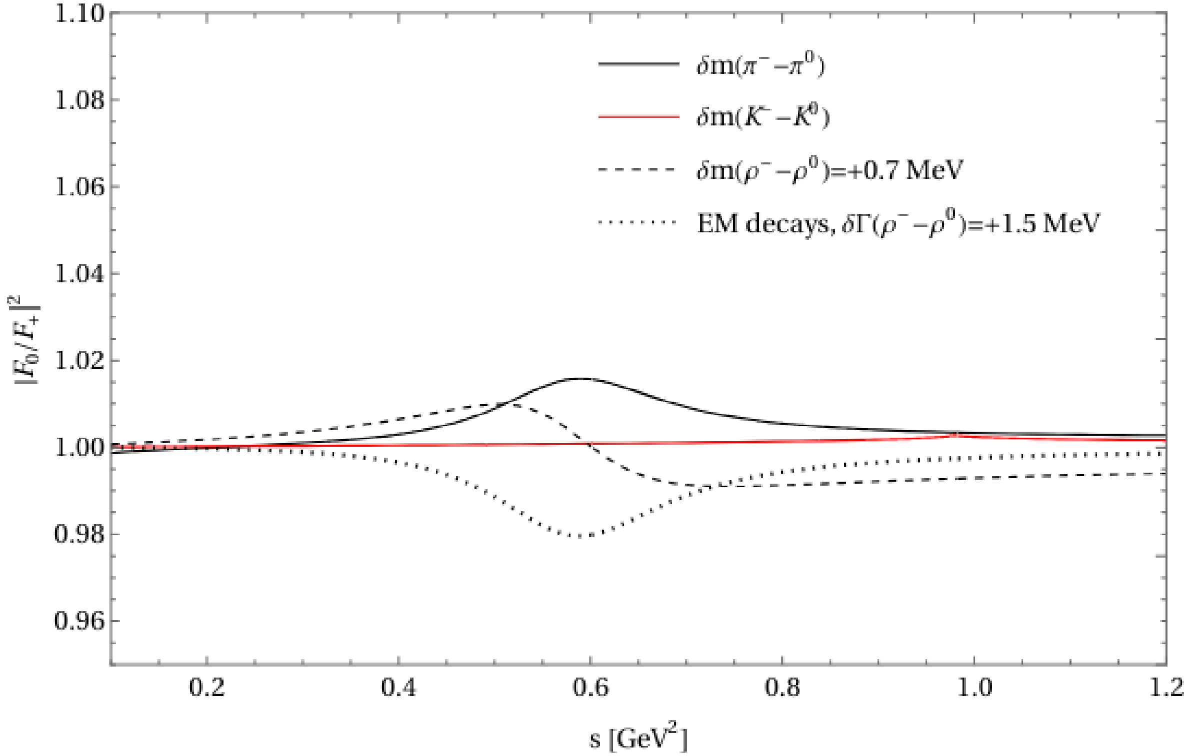

# IB corrections to $B_{\pi\pi0}$

- Contributions to $B_{\pi\pi0}$ from the isospin-breaking corrections for the different models.

| Source | $\Delta\mathcal{B}_{\pi\pi}^{CVC}$ ($10^{-2}$) | | | |
|---|---|---|---|---|
| | GS | KS | GP | |
| | Davier *et al.* | | FF1 | FF2 |
| $S_{EW}$ | +0.57(1) | | +0.57(1) | |
| $G_{EM}$ | −0.07(17) | | $-0.09(^{3}_{1})$ | |
| FSR | −0.19(2) | | −0.19(2) | |
| $m_{\pi^\pm} - m_{\pi^0}$ effect on $\sigma$ | +0.19 | | +0.20 | |
| $m_{\pi^\pm} - m_{\pi^0}$ effect on $\Gamma_\rho$ | −0.22 | | −0.22 | |
| $m_{K^\pm} - m_{K^0}$ effect on $\Gamma_\rho$ | − | − | −0.02 | |
| $m_{\rho^\pm} - m_{\rho^0}$ | +0.08(8) | +0.09(8) | −0.01(1) | |
| $\rho - \omega$ interference | −0.01(1) | −0.02(1) | −0.10(1) | |
| $\pi\pi\gamma$, electromagnetic decays | +0.34(3) | +0.37(4) | +0.28(25) | +0.09(9) |
| TOTAL | +0.69(19) | +0.72(19) | +0.42(25) | $+0.23(^{10}_{9})$ |

$$\Delta\Gamma_\rho = 1.5 \pm 1.3 \text{ MeV}$$

$$\Delta\Gamma_\rho = 0.45 \pm 0.45 \text{ MeV}$$

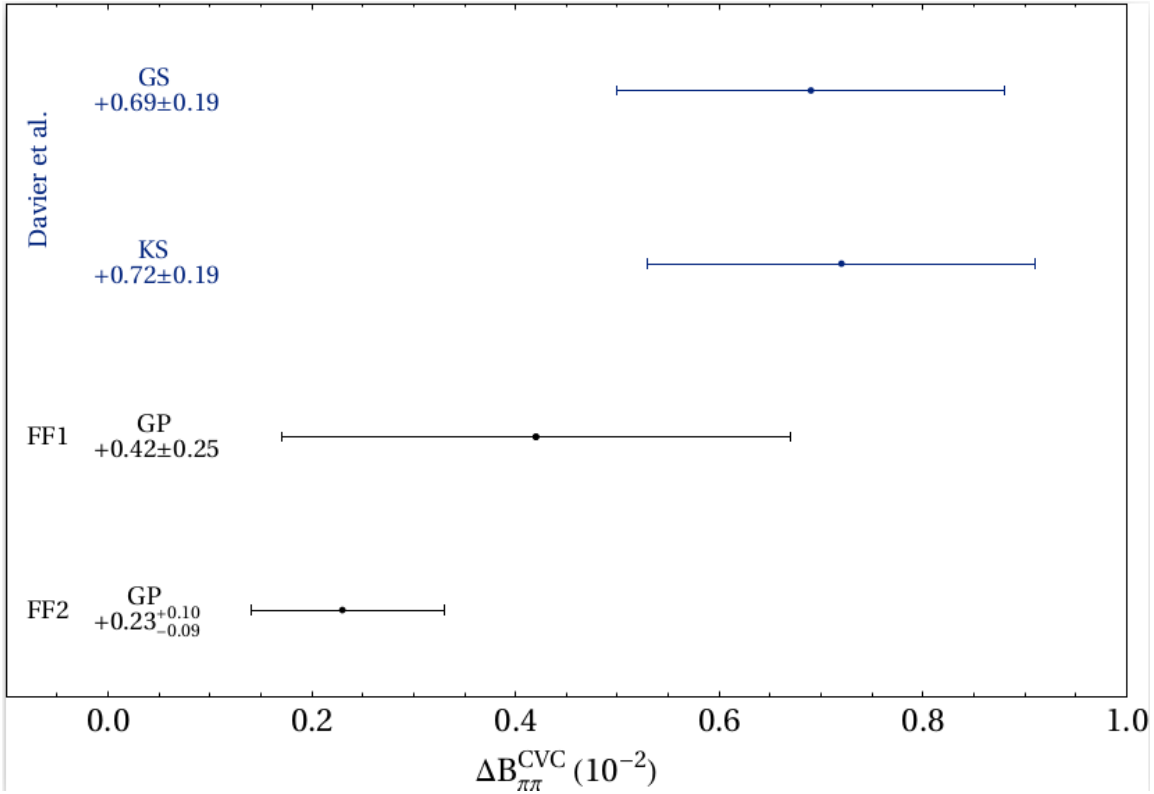

# IB corrections to $B_{\pi\pi0}$

- Contributions to $B_{\pi\pi0}$ from the **isospin-breaking corrections** for the different models.

| Source | $\Delta\mathcal{B}^{\text{CVC}}_{\pi\pi}$ $(10^{-2})$ | | | |
|---|---|---|---|---|
| | GS | KS | GP | |
| | Davier *et al.* | | FF1 | FF2 |
| $S_{\text{EW}}$ | $+0.57(1)$ | | $+0.57(1)$ | |
| $G_{\text{EM}}$ | $-0.07(17)$ | | $-0.09(^{3}_{1})$ | |
| FSR | $-0.19(2)$ | | $-0.19(2)$ | |
| $m_{\pi^\pm} - m_{\pi^0}$ effect on $\sigma$ | $+0.19$ | | $+0.20$ | |
| $m_{\pi^\pm} - m_{\pi^0}$ effect on $\Gamma_\rho$ | $-0.22$ | | $-0.22$ | |
| $m_{K^\pm} - m_{K^0}$ effect on $\Gamma_\rho$ | $-$ | $-$ | $-0.02$ | |
| $m_{\rho^\pm} - m_{\rho^0}$ | $+0.08(8)$ | $+0.09(8)$ | $-0.01(1)$ | |
| $\rho - \omega$ interference | $-0.01(1)$ | $-0.02(1)$ | $-0.10(1)$ | |
| $\pi\pi\gamma$, electromagnetic decays | $+0.34(3)$ | $+0.37(4)$ | $+0.28(25)$ | $+0.09(9)$ |
| TOTAL | $+0.69(19)$ | $+0.72(19)$ | $+0.42(25)$ | $+0.23(^{10}_{9})$ |

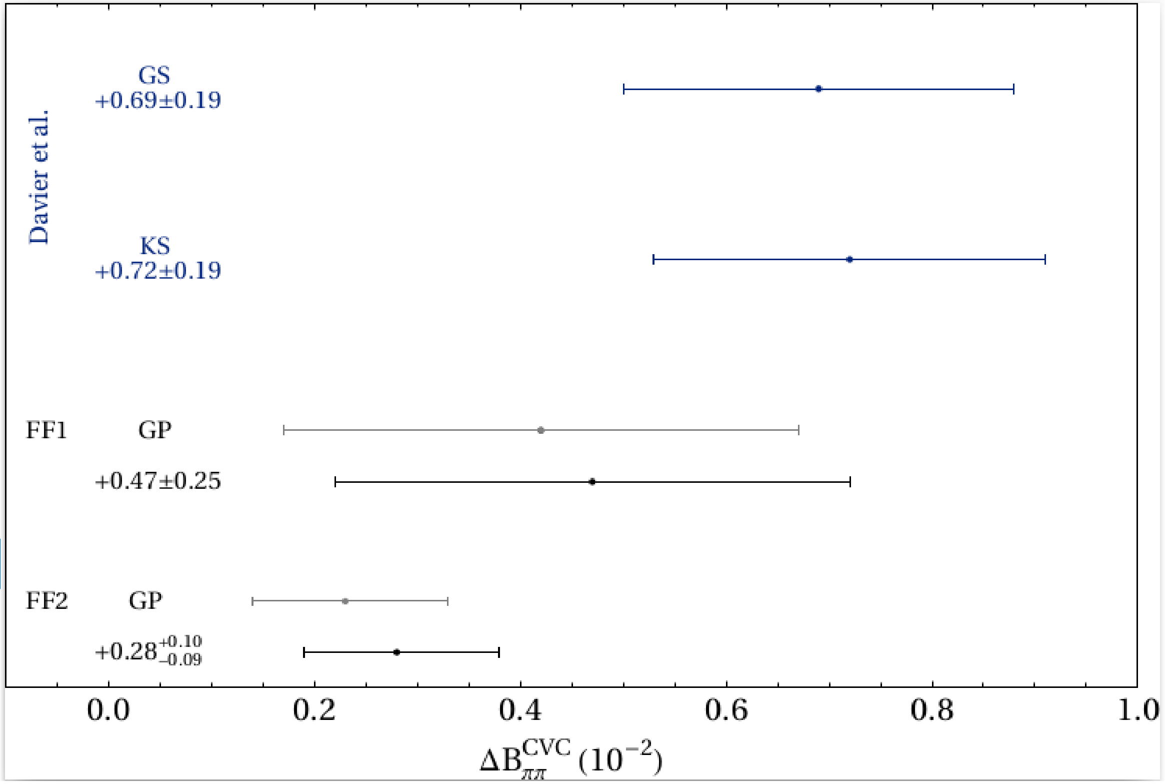


$\Delta\Gamma_\rho = 1.5 \pm 1.3$ MeV

$\Delta\Gamma_\rho = 0.45 \pm 0.45$ MeV

$|\theta_{\rho\omega}| = (3.5 \pm 0.7) \cdot 10^{-3}$ GeV$^2$

$\arg(\theta_{\rho\omega}) = (186.3 \pm 0.9)^\circ$

$\rightarrow$ $\Delta\mathcal{B}^{\text{CVC}}_{\pi\pi,\text{Mix}} = -0.05(^{2}_{1}) \cdot 10^{-2}$

# IB corrections to $a_\mu$

- Contributions to $a_\mu$ from the **isospin-breaking corrections** for the different models.

| Source | $\Delta a_\mu^{\text{had,LO}}[\pi\pi,\tau]$ $(10^{-10})$ | | | |
|---|---|---|---|---|
| | GS | KS | GP | |
| | Davier *et al.* | | FF1 | FF2 |
| $S_{\text{EW}}$ | $-12.21(0.15)$ | | $-11.96(0.15)$ | |
| $G_{\text{EM}}$ | $-1.92(0.90)$ | | $-1.71^{+0.61}_{-1.48}$ | |
| FSR | $+4.67(0.47)$ | | $+4.56(0.46)$ | |
| $m_{\pi^\pm}-m_{\pi^0}$ effect on $\sigma$ | $-7.88$ | | $-7.47$ | |
| $m_{\pi^\pm}-m_{\pi^0}$ effect on $\Gamma$ | $+4.09$ | $+4.02$ | $+4.07$ | |
| $m_{K^\pm}-m_{K^0}$ effect on $\Gamma$ | $-$ | $-$ | $+0.37$ | |
| $m_{\rho^\pm}-m_{\rho^0}$ | $+0.20^{+0.27}_{-0.19}$ | $+0.11^{+0.19}_{-0.11}$ | $+1.27^{+1.51}_{-1.45}$ | |
| $\rho-\omega$ interference | $+2.80(0.19)$ | $+2.80(0.15)$ | $+3.56^{+0.84}_{-0.80}$ | |
| $\pi\pi\gamma$ | $-5.91(0.59)$ | $-6.39(0.64)$ | $-5.14(4.45)$ | $-1.54(1.54)$ |
| TOTAL | $-16.07(1.22)$ | $-16.70(1.23)$ | $-12.45^{+4.84}_{-5.00}$ | $-8.85^{+2.44}_{-2.75}$ |

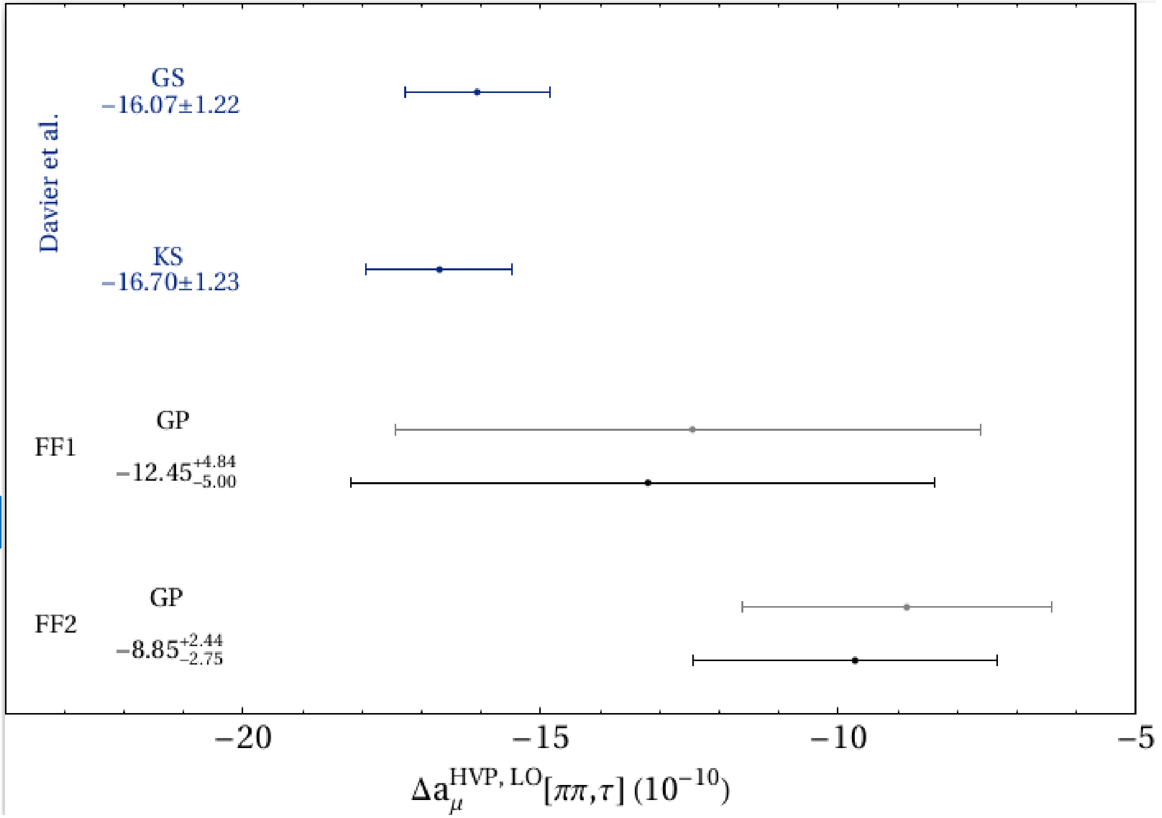


$\Delta\Gamma_\rho = 1.5 \pm 1.3$ MeV

$\Delta\Gamma_\rho = 0.45 \pm 0.45$ MeV

$|\theta_{\rho\omega}| = (3.5 \pm 0.7)\cdot 10^{-3}$ GeV$^2$

$\arg(\theta_{\rho\omega}) = (186.3 \pm 0.9)^\circ$ → $\Delta a_{\mu,\text{Mix}}^{\text{HVP}} = +2.69\binom{69}{65}\cdot 10^{-10}$

# Fit

- We perform a fit using the **e+e-** and **tau** data in the **isospin-limit** including the **rho-omega mixing**.

$$\chi^2 = \sum_k^{\mathrm{KLOE}} \left( \frac{\sigma_k^{\mathrm{th}}(e^+e^- \to \pi^+\pi^-(\gamma)) - \sigma_k^{\mathrm{exp}}(e^+e^- \to \pi^+\pi^-(\gamma))}{\delta\sigma_k^{\mathrm{exp}}(e^+e^- \to \pi^+\pi^-(\gamma))} \right)^2 + \sum_k^{\mathrm{CMD-3}} \left( \frac{|F_0^{\pi,\mathrm{th}}|_k^2 - |F_0^{\pi,\mathrm{exp}}|_k^2}{\delta|F_0^{\pi,\mathrm{exp}}|_k^2} \right)^2$$
$$+ \sum_k^{\mathrm{BABAR}} \left( \frac{\sigma_k^{\mathrm{th}}(e^+e^- \to \pi^+\pi^-(\gamma)) - \sigma_k^{\mathrm{exp}}(e^+e^- \to \pi^+\pi^-(\gamma))}{\delta\sigma_k^{\mathrm{exp}}(e^+e^- \to \pi^+\pi^-(\gamma))} \right)^2 + \sum_k^{\mathrm{Belle}} \left( \frac{|F_+^{\pi,\mathrm{th}}|_k^2 - |F_+^{\pi,\mathrm{exp}}|_k^2}{\delta|F_+^{\pi,\mathrm{exp}}|_k^2} \right)^2$$

- Additionally, we consider a modification of the GP parametrization that includes the rho' and rho'' contributions.

$$\begin{aligned} F_V(s)^{\mathrm{seed}} &= \frac{M_\rho^2 + s(\gamma e^{i\phi_1} + \delta e^{i\phi_2})}{M_\rho^2 - s - iM_\rho\Gamma_\rho(s)} \exp\left\{ \mathrm{Re}\left[ -\frac{s}{96\pi^2 F_\pi^2}\left( A_\pi(s) + \frac{1}{2}A_K(s) \right) \right] \right\} \\ &- \gamma \frac{s e^{i\phi_1}}{M_{\rho'}^2 - s - iM_{\rho'}\Gamma_{\rho'}(s)} \exp\left\{ \frac{s\Gamma_{\rho'}(M_{\rho'}^2)}{\pi M_{\rho'}^3 \sigma_\pi^3(M_{\rho'}^2)} \mathrm{Re}A_\pi(s) \right\} \\ &- \delta \frac{s e^{i\phi_2}}{M_{\rho''}^2 - s - iM_{\rho''}\Gamma_{\rho''}(s)} \exp\left\{ \frac{s\Gamma_{\rho''}(M_{\rho''}^2)}{\pi M_{\rho''}^3 \sigma_\pi^3(M_{\rho''}^2)} \mathrm{Re}A_\pi(s) \right\} , \end{aligned}$$

# Fit results for the GS model

| | BABAR12+Belle | KLOE12+Belle | KLOEc+Belle | CMD3+Belle | Global fit | Global fit |
|---|---|---|---|---|---|---|
| data points | 337 + 62 | 60 + 62 | 85 + 62 | 209 + 62 | 337+60+209+62 | 337+85+209+62 |
| $\chi^2$ | 426.9 | 432.4 | 515.7 | 268.9 | 1830.2 | 3000.9 |
| $\chi^2$/d.o.f | 1.1 | 3.9 | 3.8 | 1.0 | 2.8 | 4.4 |
| $m_\rho$ | $774.0 \pm 0.1$ MeV | $773.4 \pm 0.2$ MeV | $773.5 \pm 0.1$ MeV | $773.4 \pm 0.1$ MeV | $773.5 \pm 0.1$ MeV | $772.9 \pm 0.1$ MeV |
| $\Gamma_\rho$ | $148.9 \pm 0.3$ MeV | $144.7 \pm 0.5$ MeV | $147.1 \pm 0.3$ MeV | $147.6 \pm 0.2$ MeV | $146.6 \pm 0.2$ MeV | $146.9 \pm 0.2$ MeV |
| $\lvert\delta_{\rho\omega}\rvert$ | $(2.1 \pm 0.0) \cdot 10^{-3}$ | $(1.9 \pm 0.1) \cdot 10^{-3}$ | $(1.8 \pm 0.0) \cdot 10^{-3}$ | $(2.0 \pm 0.0) \cdot 10^{-3}$ | $(1.9 \pm 0.0) \cdot 10^{-3}$ | $(2.0 \pm 0.0) \cdot 10^{-3}$ |
| $\arg[\delta_{\rho\omega}]$ | $(10.8 \pm 1.1)^\circ$ | $(13.8 \pm 2.6)^\circ$ | $(18.2 \pm 2.6)^\circ$ | $(12.0 \pm 0.5)^\circ$ | $(10.1 \pm 0.4)^\circ$ | $(5.5 \pm 0.4)^\circ$ |
| $\lvert\delta_{\rho\phi}\rvert$ | $0^\dagger$ | $0^\dagger$ | $0^\dagger$ | $(2.2 \pm 0.2) \cdot 10^{-4}$ | $(1.5 \pm 0.2) \cdot 10^{-4}$ | $(1.4 \pm 0.2) \cdot 10^{-4}$ |
| $\arg[\delta_{\rho\phi}]$ | – | – | – | $(83.8 \pm 5.9)^\circ$ | $(68.4 \pm 7.8)^\circ$ | $(46.6 \pm 8.6)^\circ$ |
| $m_{\rho'}$ | $1460.9 \pm 5.9$ MeV | $1412.9 \pm 7.8$ MeV | $1398.9 \pm 6.7$ MeV | $1459.0 \pm 7.0$ MeV | $1433.3 \pm 4.8$ MeV | $1443.7 \pm 5.2$ MeV |
| $\Gamma_{\rho'}$ | $444 \pm 14$ MeV | $441 \pm 20$ MeV | $445 \pm 20$ MeV | $450 \pm 20$ MeV | $403 \pm 12$ MeV | $391 \pm 11$ MeV |
| $\mathrm{Re}[c_{\rho'}]$ | $-0.12 \pm 0.00$ | $-0.11 \pm 0.00$ | $-0.11 \pm 0.01$ | $-0.10 \pm 0.00$ | $-0.09 \pm 0.00$ | $-0.11 \pm 0.00$ |
| $\mathrm{Im}[c_{\rho'}]$ | $-0.03 \pm 0.01$ | $0.03 \pm 0.01$ | $-0.26 \pm 0.02$ | $-0.20 \pm 0.02$ | $-0.17 \pm 0.01$ | $-0.02 \pm 0.00$ |
| $m_{\rho''}$ | $1806.7 \pm 9.7$ MeV | $1730^\dagger$ MeV | $1730^\dagger$ MeV | $1730^\dagger$ MeV | $1784.8 \pm 10.5$ MeV | $1816.8 \pm 9.2$ MeV |
| $\Gamma_{\rho''}$ | $273 \pm 16$ MeV | $260^\dagger$ MeV | $260^\dagger$ MeV | $260^\dagger$ MeV | $245 \pm 14$ MeV | $245 \pm 16$ MeV |
| $\mathrm{Re}[c_{\rho''}]$ | $(2.9 \pm 0.5) \cdot 10^{-2}$ | $(4.9 \pm 0.6) \cdot 10^{-2}$ | $(-7.7 \pm 0.7) \cdot 10^{-2}$ | $(-7.5 \pm 0.6) \cdot 10^{-2}$ | $(-6.6 \pm 0.6) \cdot 10^{-2}$ | $(2.1 \pm 0.4) \cdot 10^{-2}$ |
| $\mathrm{Im}[c_{\rho''}]$ | $(4.5 \pm 0.3) \cdot 10^{-2}$ | $(1.7 \pm 0.3) \cdot 10^{-2}$ | $(-1.7 \pm 0.6) \cdot 10^{-3}$ | $(5.8 \pm 6.7) \cdot 10^{-3}$ | $(-2.9 \pm 0.4) \cdot 10^{-2}$ | $(4.0 \pm 0.2) \cdot 10^{-2}$ |

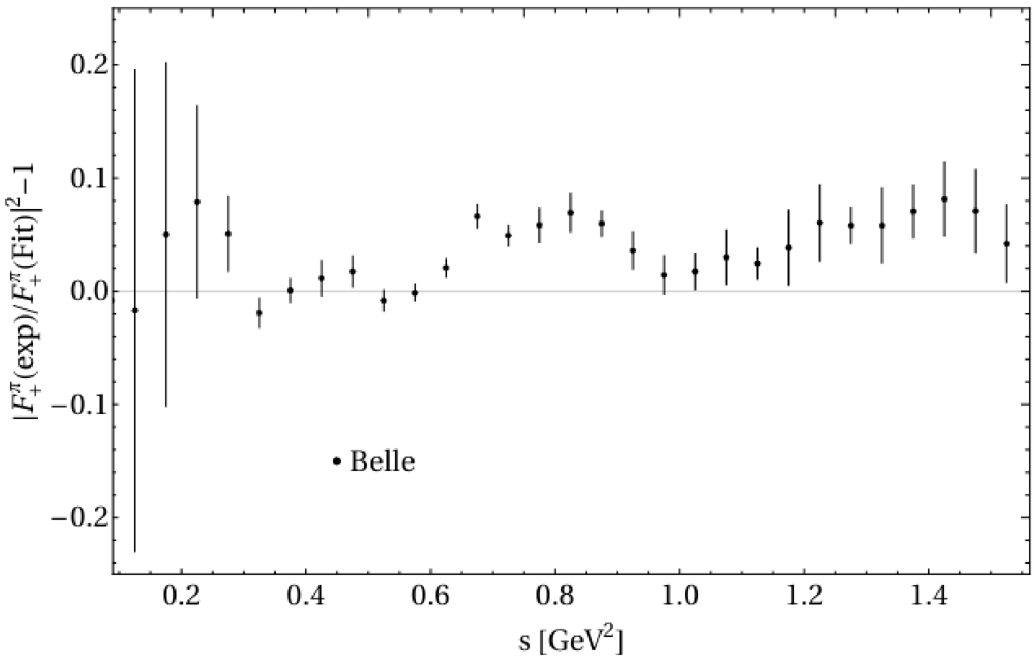
Belle
$|F_+^\pi(\text{exp})/F_+^\pi(\text{Fit})|^2-1$
s [GeV$^2$]

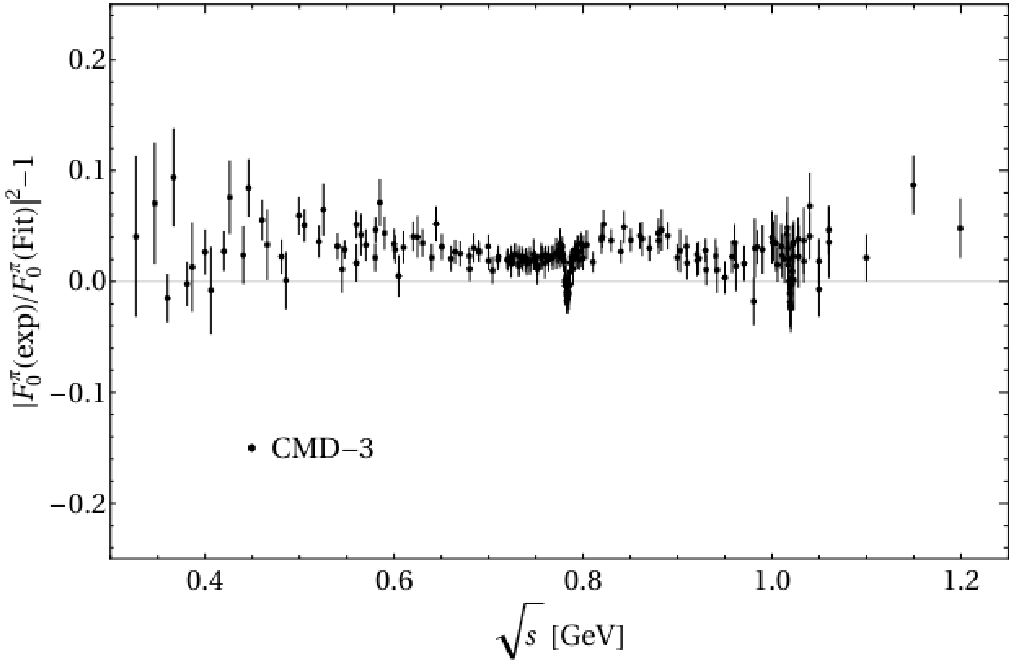
CMD−3
$|F_0^\pi(\text{exp})/F_0^\pi(\text{Fit})|^2-1$
$\sqrt{s}$ [GeV]

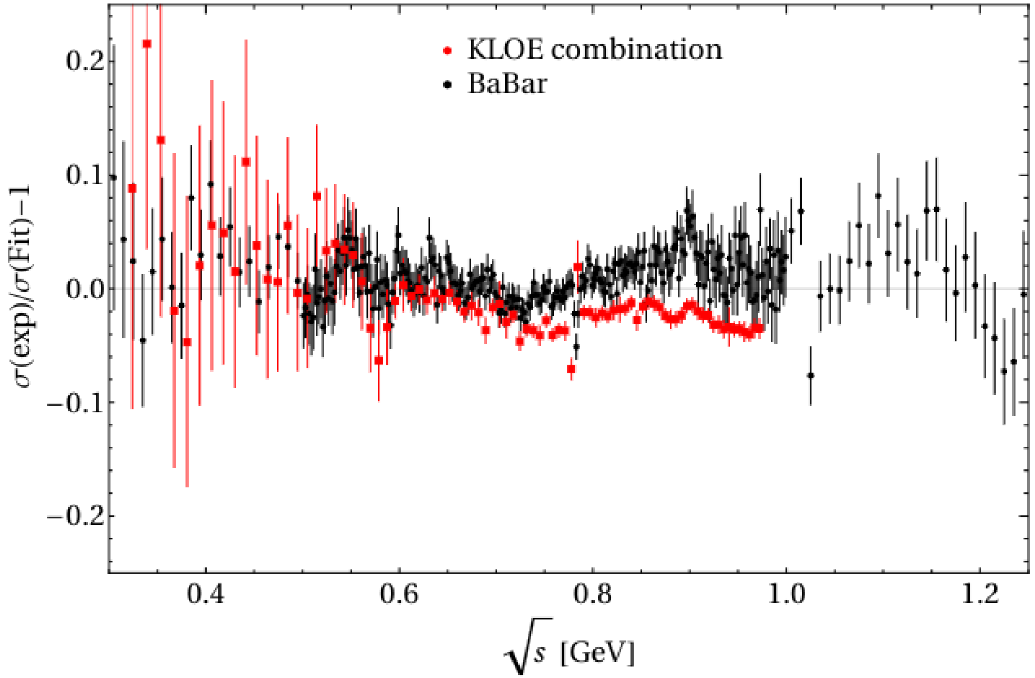
KLOE combination
BaBar
$\sigma(\text{exp})/\sigma(\text{Fit})-1$
$\sqrt{s}$ [GeV]

# Fit results for the KS model

| | BABAR12+Belle | KLOE12+Belle | KLOEc+Belle | CMD3+Belle | Global fit | Global fit |
|---|---|---|---|---|---|---|
| data points | 337 + 62 | 60 + 62 | 85 + 62 | 209 + 62 | 337+60+209+62 | 337+85+209+62 |
| $\chi^2$ | 518.4 | 496.3 | 668.3 | 614.8 | 2270.6 | 3419.5 |
| $\chi^2$/d.o.f | 1.3 | 4.4 | 4.9 | 2.4 | 3.5 | 5.0 |
| $m_\rho$ | $772.3 \pm 0.1$ MeV | $771.8 \pm 0.2$ MeV | $771.6 \pm 0.1$ MeV | $771.4 \pm 0.1$ MeV | $771.8 \pm 0.1$ MeV | $771.5 \pm 0.1$ MeV |
| $\Gamma_\rho$ | $147.5 \pm 0.3$ MeV | $142.5 \pm 0.4$ MeV | $145.0 \pm 0.3$ MeV | $146.0 \pm 0.2$ MeV | $145.5 \pm 0.2$ MeV | $145.7 \pm 0.2$ MeV |
| $\lvert\delta_{\rho\omega}\rvert$ | $(1.9 \pm 0.0) \cdot 10^{-3}$ | $(1.7 \pm 0.1) \cdot 10^{-3}$ | $(1.7 \pm 0.0) \cdot 10^{-3}$ | $(2.0 \pm 0.0) \cdot 10^{-3}$ | $(1.9 \pm 0.0) \cdot 10^{-3}$ | $(1.9 \pm 0.0) \cdot 10^{-3}$ |
| $\arg[\delta_{\rho\omega}]$ | $(11.7 \pm 1.1)^\circ$ | $(17.6 \pm 2.9)^\circ$ | $(17.6 \pm 2.7)^\circ$ | $(11.3 \pm 0.5)^\circ$ | $(9.5 \pm 0.4)^\circ$ | $(6.5 \pm 0.4)^\circ$ |
| $\lvert\delta_{\rho\phi}\rvert$ | $0^\dagger$ | $0^\dagger$ | $0^\dagger$ | $(2.8 \pm 0.2) \cdot 10^{-4}$ | $(1.7 \pm 0.2) \cdot 10^{-4}$ | $(1.4 \pm 0.2) \cdot 10^{-4}$ |
| $\arg[\delta_{\rho\phi}]$ | – | – | – | $(87.0 \pm 4.9)^\circ$ | $(78.9 \pm 7.5)^\circ$ | $(73.2 \pm 8.1)^\circ$ |
| $m_{\rho'}$ | $1536.1 \pm 9.5$ MeV | $1425.2 \pm 8.3$ MeV | $1476.7 \pm 8.0$ MeV | $1575.8 \pm 10.9$ MeV | $1564.9 \pm 9.3$ MeV | $1547.5 \pm 8.1$ MeV |
| $\Gamma_{\rho'}$ | $538 \pm 18$ MeV | $471 \pm 18$ MeV | $474 \pm 14$ MeV | $717 \pm 23$ MeV | $450 \pm 17$ MeV | $447 \pm 16$ MeV |
| $\mathrm{Re}[c_{\rho'}]$ | $-0.13 \pm 0.01$ | $-0.13 \pm 0.00$ | $-0.13 \pm 0.00$ | $-0.23 \pm 0.01$ | $(3.6 \pm 3.3) \cdot 10^{-2}$ | $(-0.6 \pm 2.7) \cdot 10^{-2}$ |
| $\mathrm{Im}[c_{\rho'}]$ | $-0.28 \pm 0.02$ | $-0.19 \pm 0.02$ | $-0.17 \pm 0.02$ | $-0.23 \pm 0.01$ | $-0.28 \pm 0.03$ | $-0.27 \pm 0.02$ |
| $m_{\rho''}$ | $1831.4 \pm 12.6$ MeV | $1730^\dagger$ MeV | $1730^\dagger$ MeV | $1730^\dagger$ MeV | $1865.8 \pm 20.1$ MeV | $1868.2 \pm 16.3$ MeV |
| $\Gamma_{\rho''}$ | $442 \pm 33$ MeV | $260^\dagger$ MeV | $260^\dagger$ MeV | $260^\dagger$ MeV | $721 \pm 53$ MeV | $650 \pm 50$ MeV |
| $\mathrm{Re}[c_{\rho''}]$ | $-(8.4 \pm 1.5) \cdot 10^{-2}$ | $(-6.0 \pm 0.6) \cdot 10^{-2}$ | $(-5.0 \pm 0.7) \cdot 10^{-2}$ | $(1.9 \pm 1.0) \cdot 10^{-2}$ | $-0.25 \pm 0.04$ | $-0.20 \pm 0.03$ |
| $\mathrm{Im}[c_{\rho''}]$ | $0.13 \pm 0.01$ | $(3.1 \pm 0.7) \cdot 10^{-2}$ | $(4.6 \pm 0.7) \cdot 10^{-2}$ | $0.10 \pm 0.00$ | $0.13 \pm 0.02$ | $0.12 \pm 0.01$ |

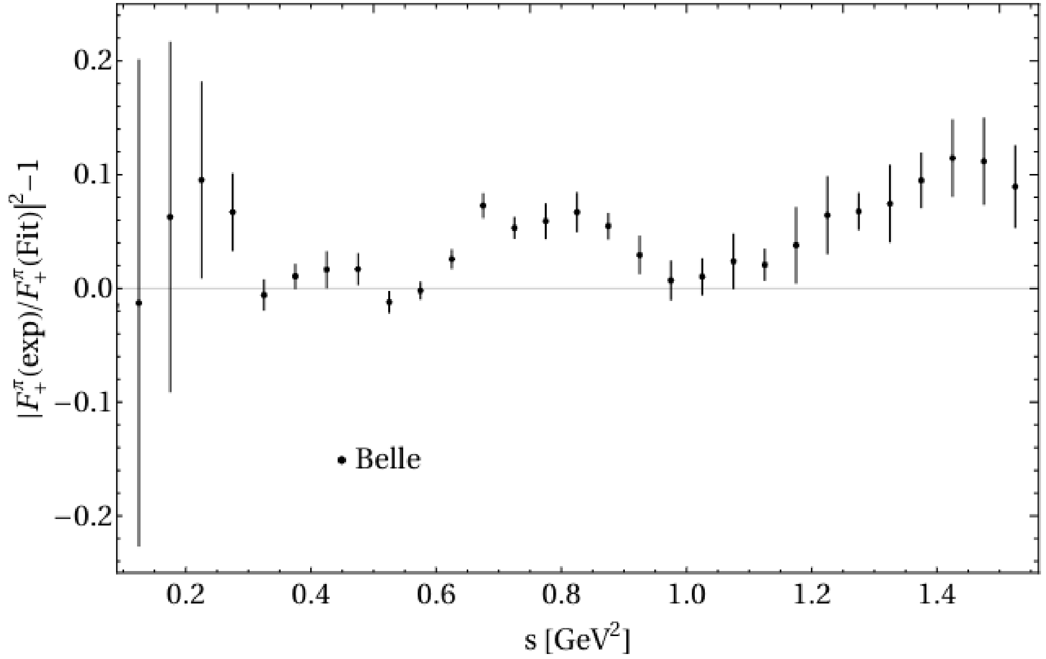
Belle
$|F_+^\pi(\exp)/F_+^\pi(\mathrm{Fit})|^2-1$
s [GeV$^2$]

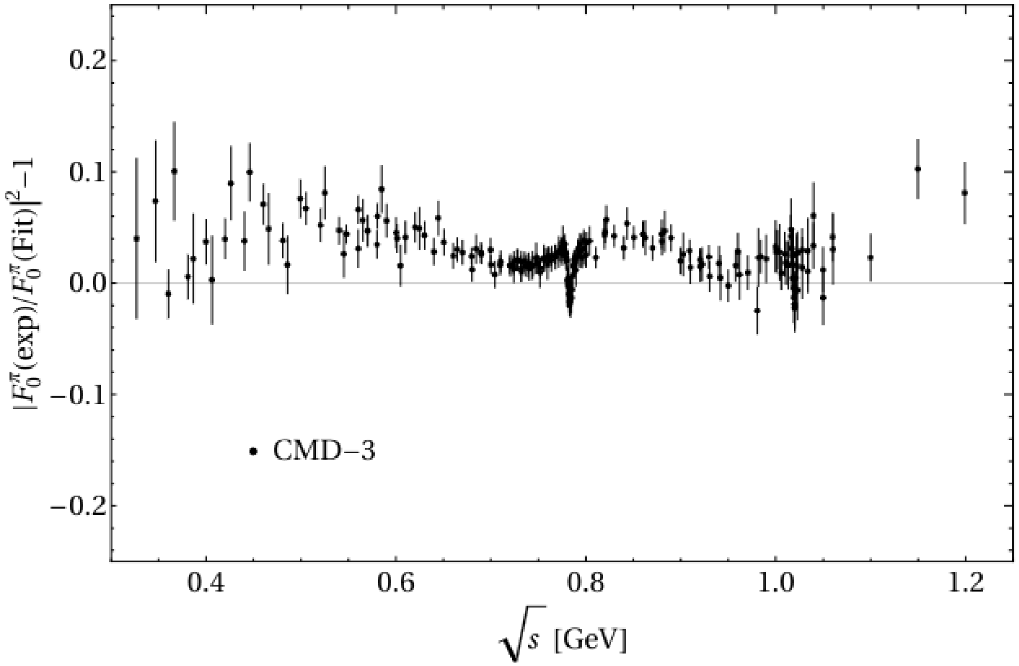
CMD−3
$|F_0^\pi(\exp)/F_0^\pi(\mathrm{Fit})|^2-1$
$\sqrt{s}$ [GeV]

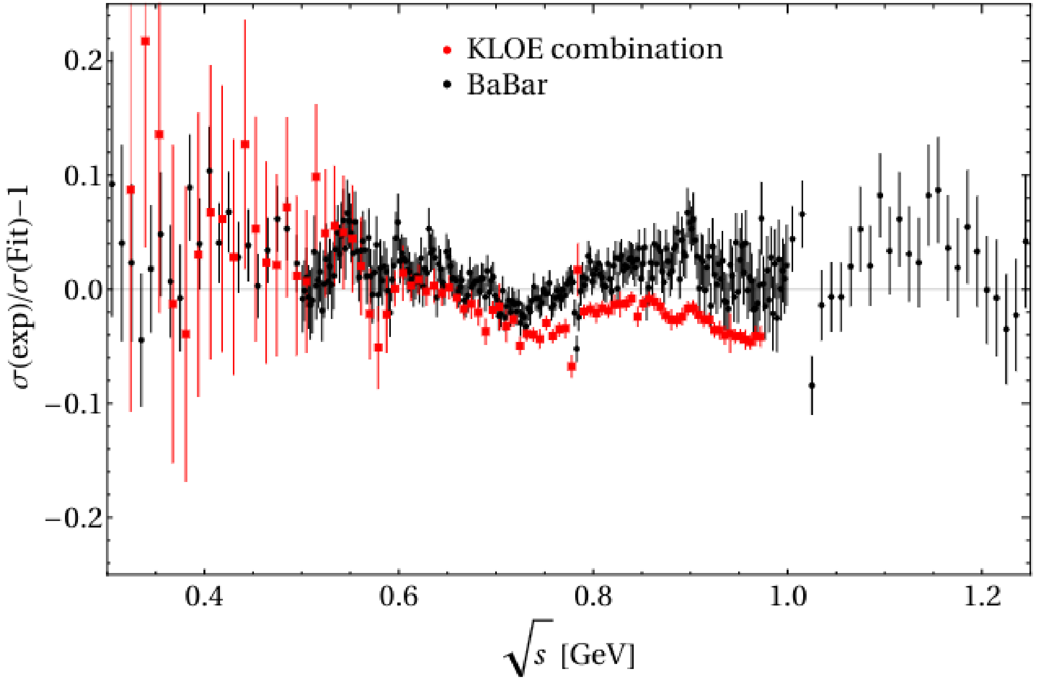
KLOE combination
BaBar
$\sigma(\exp)/\sigma(\mathrm{Fit})-1$
$\sqrt{s}$ [GeV]

# Fit results for the GP model

| | BABAR12+Belle | KLOE12+Belle | KLOEc+Belle | CMD3+Belle | Global Fit | Global Fit |
|---|---|---|---|---|---|---|
| data points | 270 + 19 | 60 + 19 | 85 + 19 | 172 + 19 | 270+60+172+19 | 270+85+172+19 |
| $\chi^2$ | 1671.7 | 572.5 | 848.9 | 3279.6 | 4887.1 | 5065.4 |
| $\chi^2$/d.o.f | 5.8 | 7.5 | 8.4 | 17.4 | 9.4 | 9.3 |
| $m_\rho$ | $776.0 \pm 0.1$ MeV | $777.4 \pm 0.1$ MeV | $776.0 \pm 0.1$ MeV | $774.8 \pm 0.1$ MeV | $775.5 \pm 0.1$ MeV | $775.4 \pm 0.1$ MeV |
| $\mathrm{Re}[\delta_{\rho\omega}] = \mathrm{Re}\left[-\frac{\theta_{\rho\omega}}{3m_\rho}\right]$ | $(2.5 \pm 0.0) \cdot 10^{-3}$ | $(2.6 \pm 0.1) \cdot 10^{-3}$ | $(2.5 \pm 0.1) \cdot 10^{-3}$ | $(2.5 \pm 0.0) \cdot 10^{-3}$ | $(2.5 \pm 0.0) \cdot 10^{-3}$ | $(2.5 \pm 0.0) \cdot 10^{-3}$ |
| $\mathrm{Im}[\delta_{\rho\omega}] = \mathrm{Im}\left[-\frac{\theta_{\rho\omega}}{3m_\rho}\right]$ | $(0.3 \pm 0.0) \cdot 10^{-3}$ | $(0.4 \pm 0.1) \cdot 10^{-3}$ | $(0.8 \pm 0.1) \cdot 10^{-3}$ | $(0.1 \pm 0.0) \cdot 10^{-3}$ | $(0.1 \pm 0.0) \cdot 10^{-3}$ | $(0.1 \pm 0.0) \cdot 10^{-3}$ |
| $\lvert\delta_{\rho\omega}\rvert$ | $(2.6 \pm 0.0) \cdot 10^{-3}$ | $(2.6 \pm 0.1) \cdot 10^{-3}$ | $(2.7 \pm 0.1) \cdot 10^{-3}$ | $(2.5 \pm 0.0) \cdot 10^{-3}$ | $(2.5 \pm 0.0) \cdot 10^{-3}$ | $(2.5 \pm 0.0) \cdot 10^{-3}$ |
| $\arg[\delta_{\rho\omega}]$ | $(6.2 \pm 0.9)^\circ$ | $(9.2 \pm 2.1)^\circ$ | $(18.6 \pm 1.8)^\circ$ | $(1.4 \pm 0.4)^\circ$ | $(2.6 \pm 0.3)^\circ$ | $(2.8 \pm 0.3)^\circ$ |

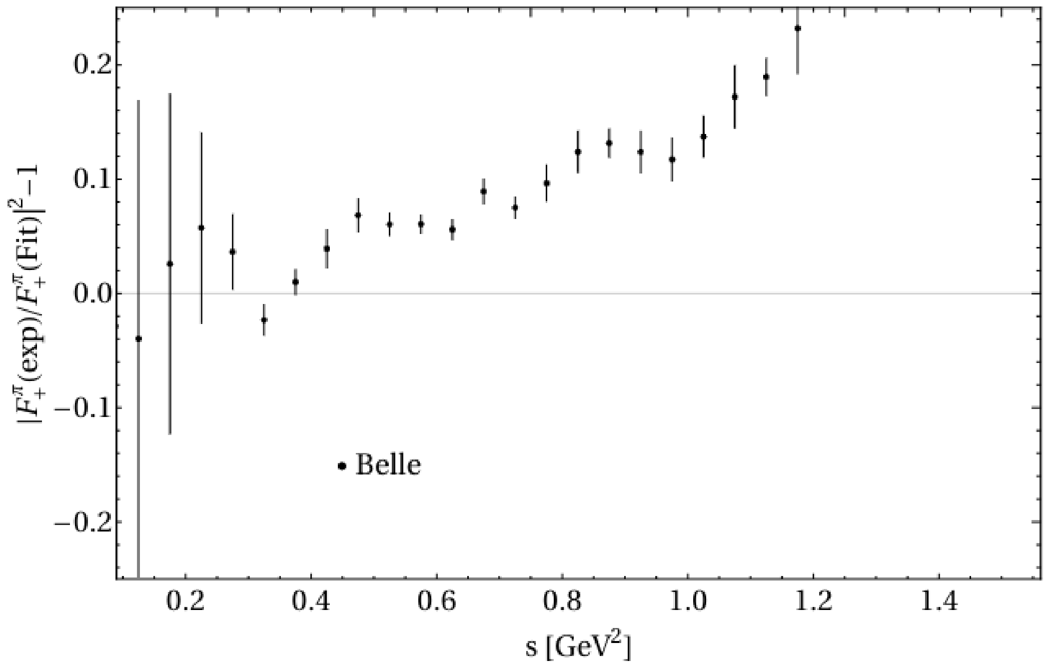

$|F_+^\pi(\exp)/F_+^\pi(\mathrm{Fit})|^2-1$
Belle
s [GeV$^2$]


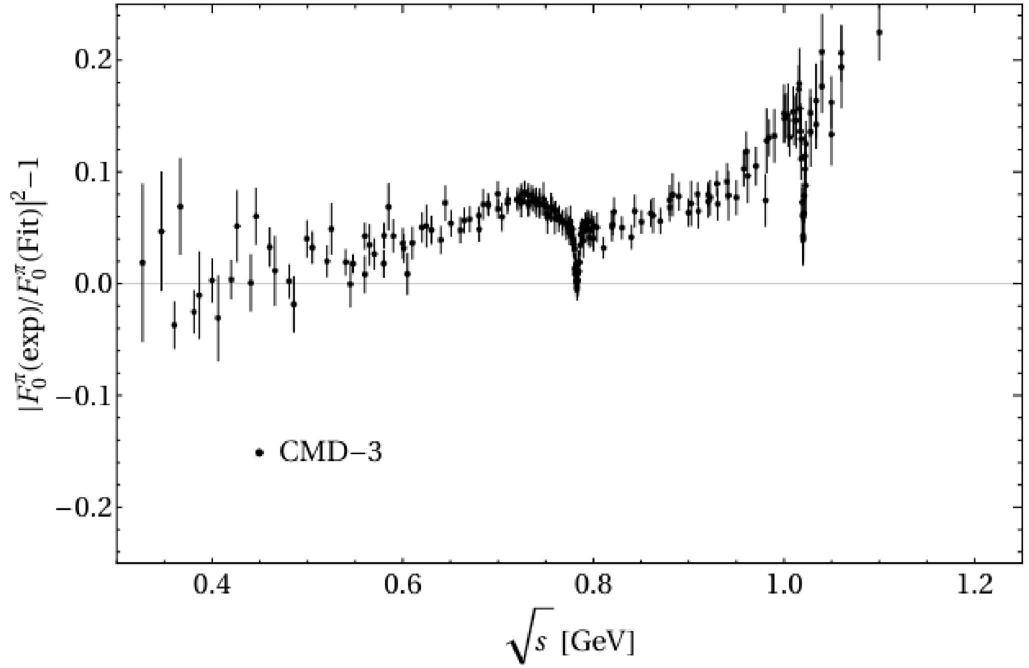

$|F_0^\pi(\exp)/F_0^\pi(\mathrm{Fit})|^2-1$
CMD−3
$\sqrt{s}$ [GeV]


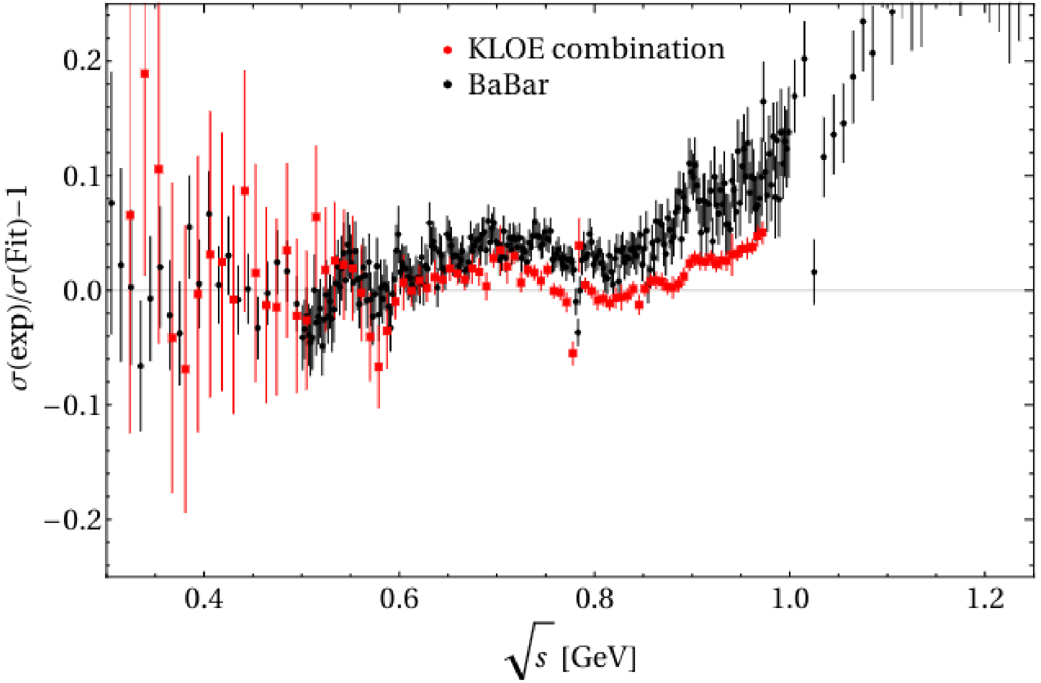

KLOE combination
BaBar
$\sigma(\exp)/\sigma(\mathrm{Fit})-1$
$\sqrt{s}$ [GeV]

# Fit results for the Seed model

| | BABAR12+Belle | KLOE12+Belle | KLOEc+Belle | CMD3+Belle | Global fit | Global fit |
|---|---|---|---|---|---|---|
| data points | 337 + 62 | 60 + 62 | 85 + 62 | 209 + 62 | 337+60+209+62 | 337+85+209+62 |
| $\chi^2$ | 556.4 | 432.9 | 539.4 | 222.5 | 1662.7 | 2514.5 |
| $\chi^2$/d.o.f | 1.4 | 3.8 | 3.9 | 0.9 | 2.5 | 3.7 |
| $m_\rho$ | $774.6 \pm 0.1$ MeV | $774.1 \pm 0.2$ MeV | $773.7 \pm 0.1$ MeV | $773.6 \pm 0.1$ MeV | $773.8 \pm 0.1$ MeV | $773.5 \pm 0.1$ MeV |
| $\lvert\delta_{\rho\omega}\rvert$ | $(2.5 \pm 0.0) \cdot 10^{-3}$ | $(2.4 \pm 0.1) \cdot 10^{-3}$ | $(2.3 \pm 0.1) \cdot 10^{-3}$ | $(2.5 \pm 0.0) \cdot 10^{-3}$ | $(2.4 \pm 0.0) \cdot 10^{-3}$ | $(2.4 \pm 0.0) \cdot 10^{-3}$ |
| $\arg[\delta_{\rho\omega}]$ | $(13.5 \pm 1.0)^\circ$ | $(10.7 \pm 2.5)^\circ$ | $(16.8 \pm 2.3)^\circ$ | $(11.3 \pm 0.4)^\circ$ | $(9.1 \pm 0.4)^\circ$ | $(6.5 \pm 0.4)^\circ$ |
| $\lvert\delta_{\rho\phi}\rvert$ | $0^\dagger$ | $0^\dagger$ | $0^\dagger$ | $(2.8 \pm 0.2) \cdot 10^{-4}$ | $(2.0 \pm 0.2) \cdot 10^{-4}$ | $(2.1 \pm 0.3) \cdot 10^{-4}$ |
| $\arg[\delta_{\rho\phi}]$ | – | – | – | $(63.1 \pm 5.4)^\circ$ | $(58.2 \pm 6.3)^\circ$ | $(40.9 \pm 6.7)^\circ$ |
| $m_{\rho'}$ | $1397.2 \pm 8.3$ MeV | $1413.8 \pm 11.7$ MeV | $1406.3 \pm 12.1$ MeV | $1449.2 \pm 11.5$ MeV | $1414.5 \pm 3.3$ MeV | $1369.4 \pm 7.8$ MeV |
| $\Gamma_{\rho'}$ | $324 \pm 15$ MeV | $386 \pm 28$ MeV | $447 \pm 33$ MeV | $385 \pm 28$ MeV | $231 \pm 7$ MeV | $343 \pm 16$ MeV |
| $\mathrm{Re}[c_{\rho'}]$ | $(9.2 \pm 0.5) \cdot 10^{-2}$ | $0.11 \pm 0.01$ | $0.12 \pm 0.00$ | $0.13 \pm 0.01$ | $(3.1 \pm 0.5) \cdot 10^{-2}$ | $(7.9 \pm 0.5) \cdot 10^{-2}$ |
| $\mathrm{Im}[c_{\rho'}]$ | $(-5.1 \pm 0.6) \cdot 10^{-2}$ | $(-8.8 \pm 0.9) \cdot 10^{-2}$ | $-0.12 \pm 0.01$ | $(-4.7 \pm 0.8) \cdot 10^{-2}$ | $0.19 \pm 0.01$ | $(-7.2 \pm 0.5) \cdot 10^{-2}$ |
| $m_{\rho''}$ | $1721.7 \pm 10.5$ MeV | $1730^\dagger$ MeV | $1730^\dagger$ MeV | $1730^\dagger$ MeV | $1793.4 \pm 6.7$ MeV | $1698.2 \pm 10.6$ MeV |
| $\Gamma_{\rho''}$ | $211 \pm 12$ MeV | $260^\dagger$ MeV | $260^\dagger$ MeV | $260^\dagger$ MeV | $120 \pm 6$ MeV | $203 \pm 10$ MeV |
| $\mathrm{Re}[c_{\rho''}]$ | $(-8.1 \pm 0.5) \cdot 10^{-2}$ | $-0.11 \pm 0.01$ | $-0.12 \pm 0.00$ | $-0.11 \pm 0.01$ | $(-2.7 \pm 0.4) \cdot 10^{-2}$ | $(-7.3 \pm 0.5) \cdot 10^{-2}$ |
| $\mathrm{Im}[c_{\rho''}]$ | $(2.6 \pm 0.8) \cdot 10^{-2}$ | $(4.1 \pm 0.8) \cdot 10^{-2}$ | $(9.8 \pm 0.7) \cdot 10^{-2}$ | $(2.0 \pm 0.7) \cdot 10^{-2}$ | $(4.0 \pm 0.3) \cdot 10^{-2}$ | $(4.5 \pm 0.8) \cdot 10^{-2}$ |

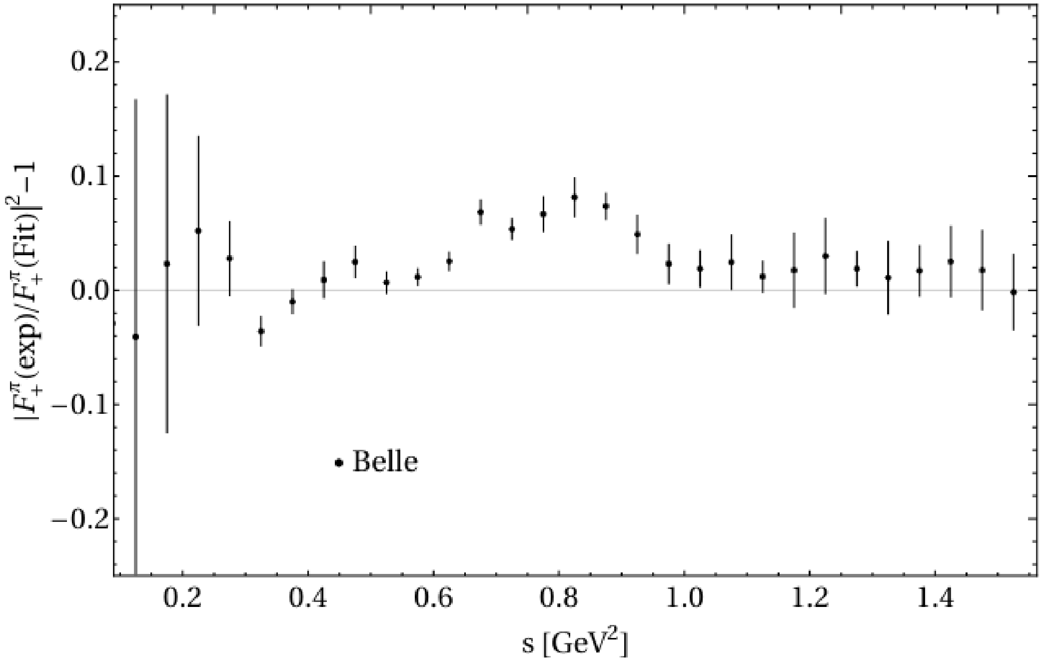
$|F_+^\pi(\text{exp})/F_+^\pi(\text{Fit})|^2-1$
0.2
0.1
0.0
−0.1
−0.2
Belle
0.2
0.4
0.6
0.8
1.0
1.2
1.4
s [GeV$^2$]

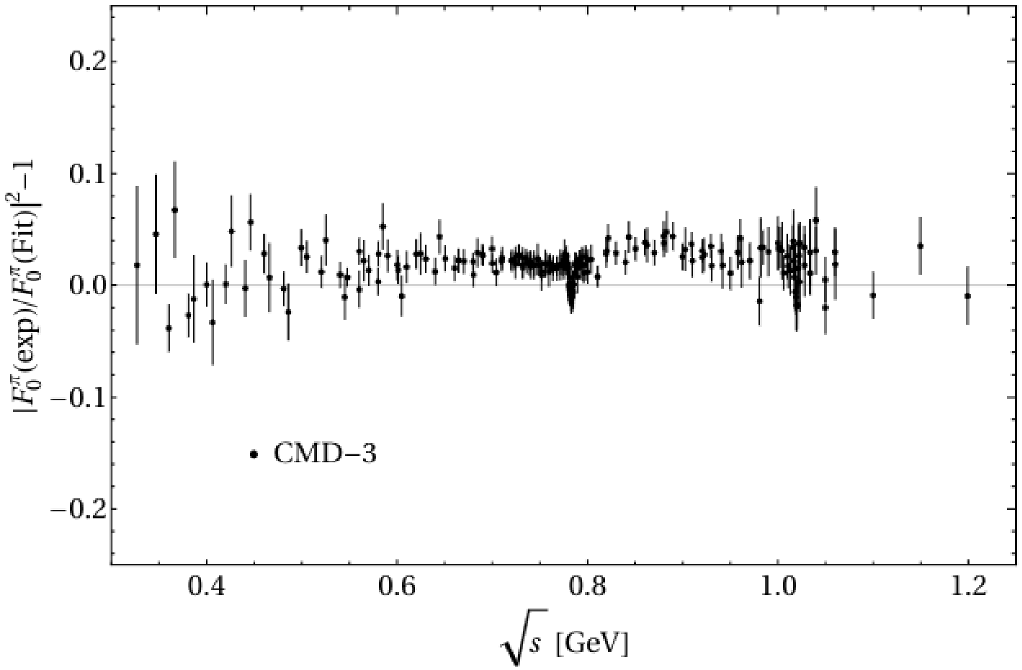
$|F_0^\pi(\text{exp})/F_0^\pi(\text{Fit})|^2-1$
0.2
0.1
0.0
−0.1
−0.2
CMD−3
0.4
0.6
0.8
1.0
1.2
$\sqrt{s}$ [GeV]

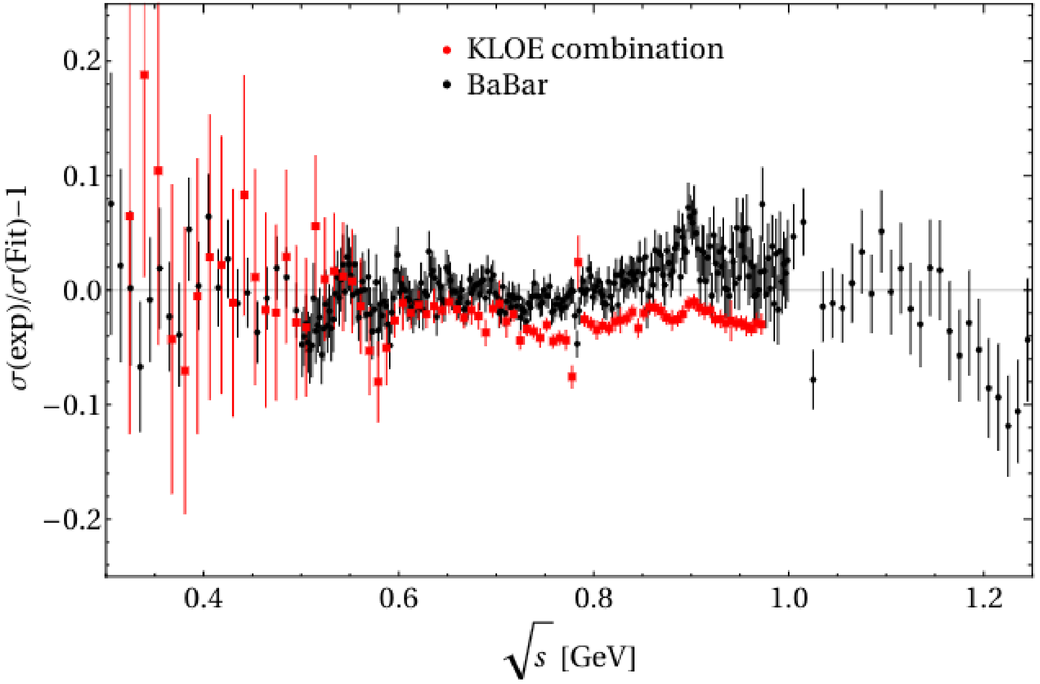
$\sigma(\text{exp})/\sigma(\text{Fit})-1$
0.2
0.1
0.0
−0.1
−0.2
KLOE combination
BaBar
0.4
0.6
0.8
1.0
1.2
$\sqrt{s}$ [GeV]

# IB corrections to $B_{\pi\pi0}$

- Contributions to $B_{\pi\pi0}$ from the isospin-breaking corrections for the different models.

| Source | $\Delta\mathcal{B}_{\pi\pi}^{\mathrm{CVC}}$ $(10^{-2})$ | | | |
|---|---|---|---|---|
| | GS | KS | GP | Seed |
| $S_{\mathrm{EW}}$ | $+0.57(1)$ | | | |
| $G_{\mathrm{EM}}$ | $-0.09(^{3}_{1})$ | | | |
| FSR | $-0.19(2)$ | | | |
| $m_{\pi^\pm} - m_{\pi^0}$ effect on $\sigma$ | $+0.20$ | | | |
| $m_{\pi^\pm} - m_{\pi^0}$ effect on $\Gamma_\rho$ | $-0.21$ | $-0.22$ | $-0.22$ | $-0.23$ |
| $m_{K^\pm} - m_{K^0}$ effect on $\Gamma_\rho$ | – | – | $-0.02$ | $-0.03$ |
| $m_{\rho^\pm} - m_{\rho^0}$ | $+0.08(8)$ | $+0.09(8)$ | $-0.02(2)$ | $-0.02(2)$ |
| $\rho - \omega$ interference | $-0.08(0)$ | $-0.09(0)$ | $-0.09(0)$ | $-0.06(0)$ |
| $\rho - \phi$ interference | $-0.00(0)$ | $-0.00(0)$ | – | $-0.00(0)$ |
| $\pi\pi\gamma$, electromagnetic decays | $+0.34(3)$ | $+0.37(4)$ | $+0.34(4)$ | $+0.34(4)$ |
| TOTAL | $+0.62(9)$ | $+0.64(^{10}_{9})$ | $+0.48(^{6}_{5})$ | $+0.49(^{6}_{5})$ |

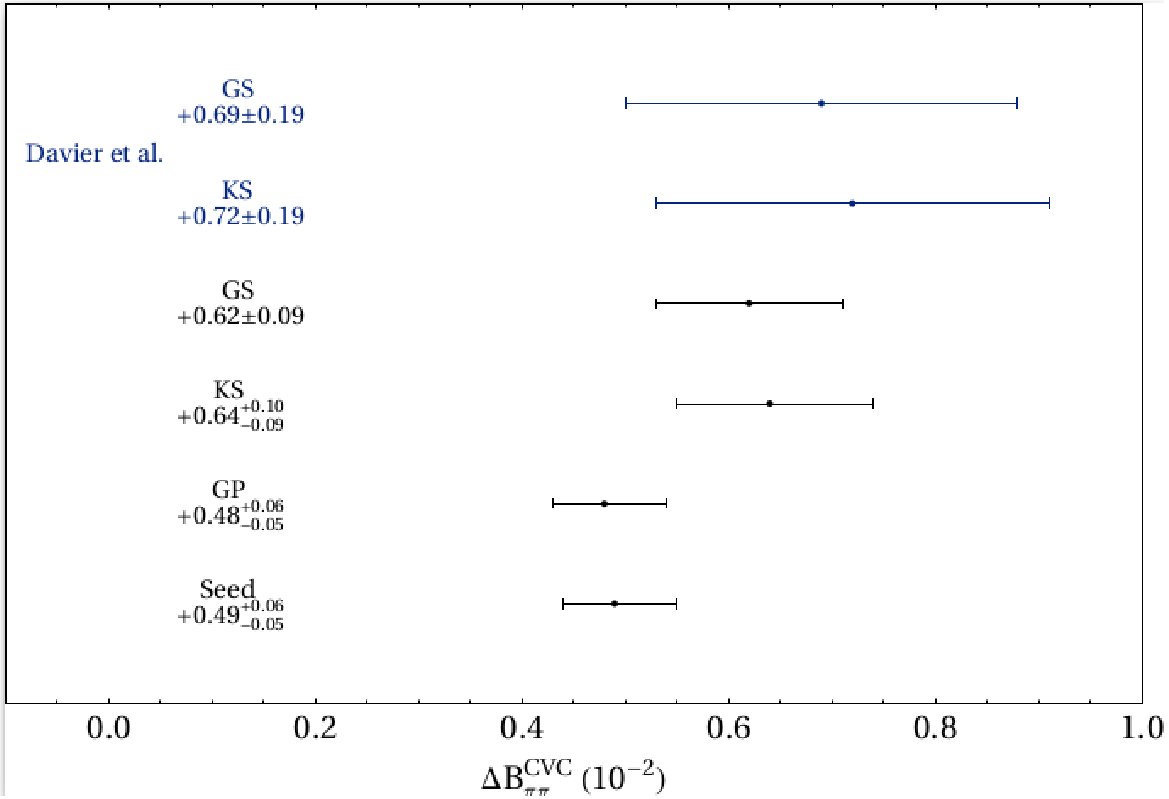

# IB corrections to $a_\mu$

- Contributions to $a_\mu$ from the **isospin-breaking corrections**.

| Source | $\Delta a_\mu^{\text{had,LO}}[\pi\pi,\tau]$ $(10^{-10})$ | | | |
|---|---|---|---|---|
| | GS | KS | GP | Seed |
| $S_{\text{EW}}$ | $-11.96(0.15)$ | | | |
| $G_{\text{EM}}$ | $-1.71^{+0.61}_{-1.48}$ | | | |
| FSR | $+4.56(0.46)$ | | | |
| $m_{\pi^\pm} - m_{\pi^0}$ effect on $\sigma$ | $-7.47$ | | | |
| $m_{\pi^\pm} - m_{\pi^0}$ effect on $\Gamma$ | $+3.74$ | $+4.12$ | $+4.07$ | $+4.13$ |
| $m_{K^\pm} - m_{K^0}$ effect on $\Gamma$ | – | – | $+0.37$ | $+0.36$ |
| $m_{\rho^\pm} - m_{\rho^0}$ | $+0.10^{+0.18}_{-0.09}$ | $-0.04^{+0.06}_{-0.00}$ | $+1.87^{+1.75}_{-1.68}$ | $+1.86^{+1.75}_{-1.68}$ |
| $\rho - \omega$ interference | $+3.84(0.08)$ | $+4.00(0.08)$ | $+4.33(0.07)$ | $+3.57(0.07)$ |
| $\rho - \phi$ interference | $+0.09(0.03)$ | $+0.03(0.03)$ | – | $+0.13(0.03)$ |
| $\pi\pi\gamma$ | $-6.09(0.67)$ | $-6.68(0.74)$ | $-6.19(0.68)$ | $-6.21(0.68)$ |
| TOTAL | $-14.90^{+1.05}_{-1.70}$ | $-15.15^{+1.08}_{-1.73}$ | $-12.13^{+2.03}_{-2.39}$ | $-12.74^{+2.03}_{-2.39}$ |

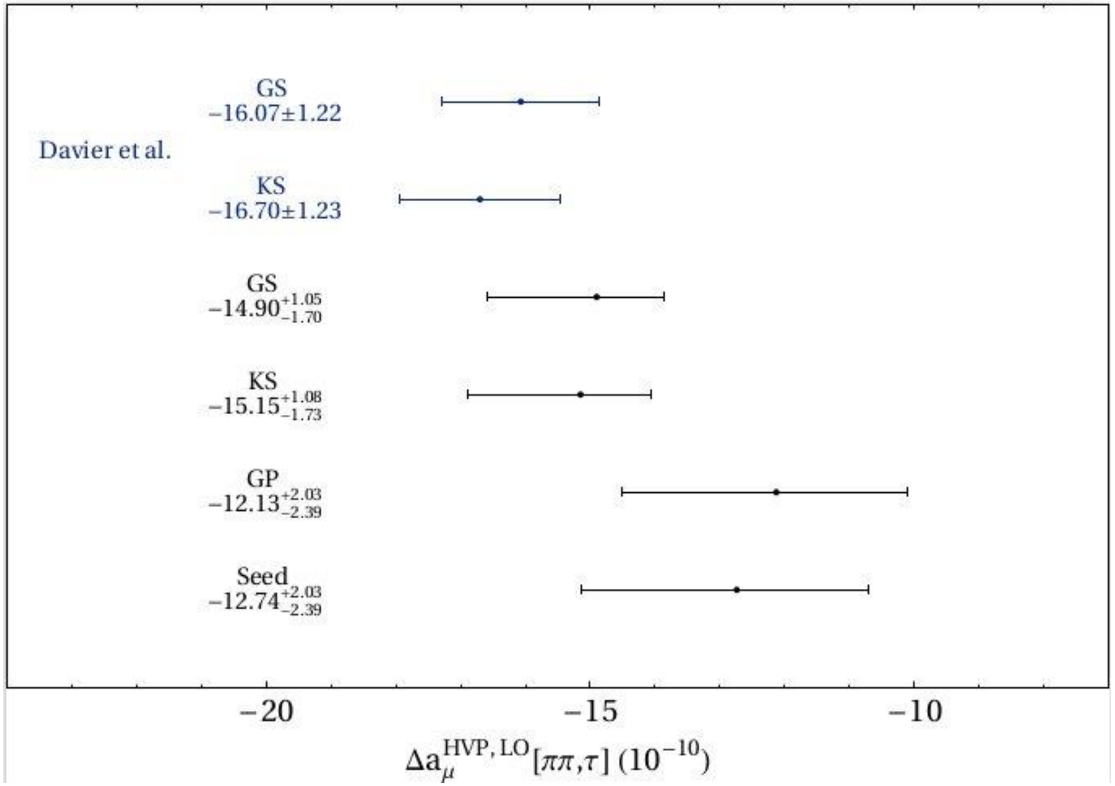

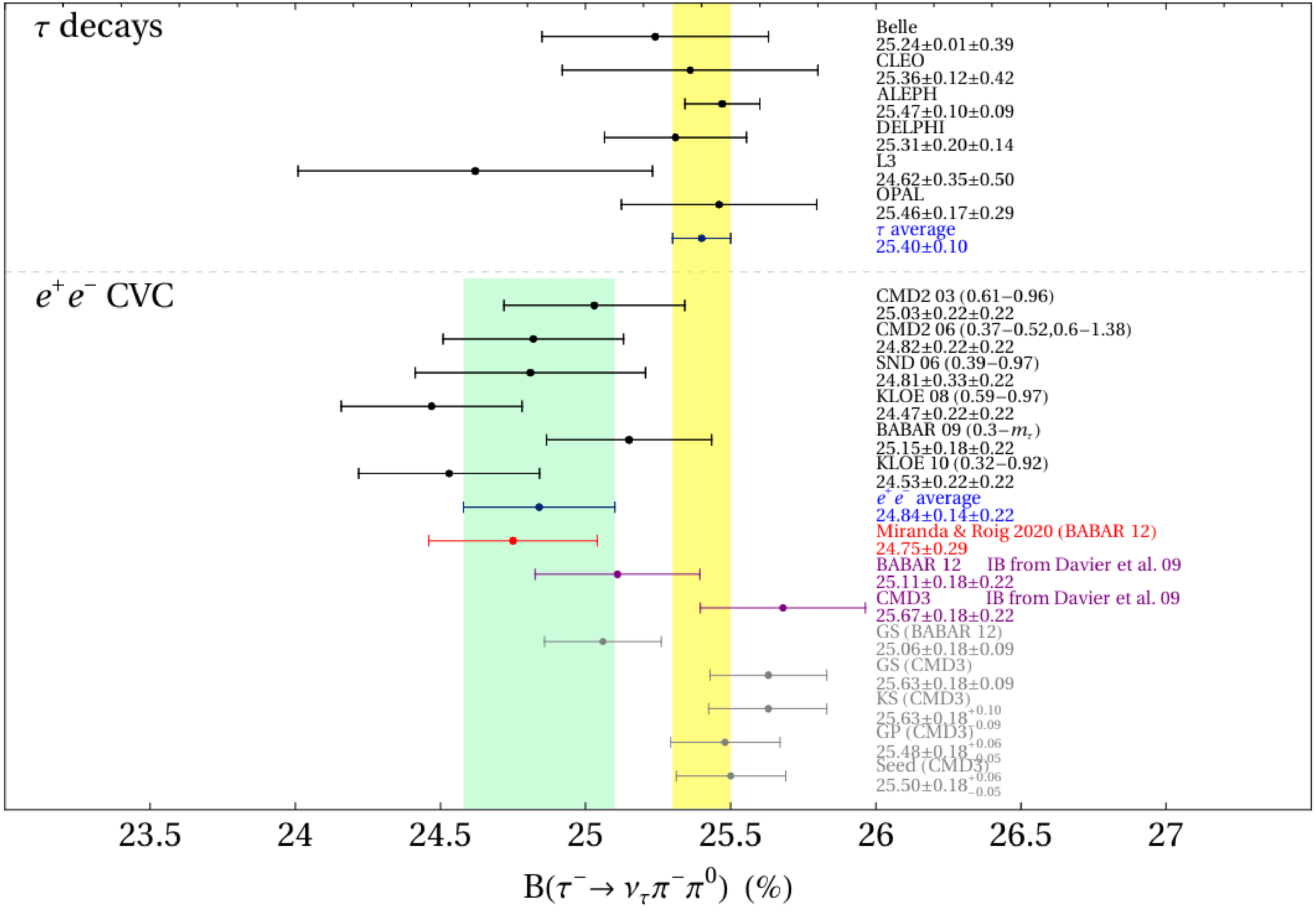


There is a **good agreement** between the $e^+e^-$ **prediction** via CVC and **measurement**.

# Conclusions

- An important independent **cross-check** is provided by the **tau branching fraction**, another key quantity which can be directly **measured**.
- There is a **good agreement** between prediction and experiment for **BaBar** and **CMD-3**.
- In light of the puzzling situation regarding the **IB-breaking corrections** in the **tau-based** method, there is a significant effort in the **lattice** in this regard.
- In this perplexing scenario, we insist about utilizing **tau input** for the dominant **di-pion** channel.

# References


- V. Cirigliano, G. Ecker and H. Neufeld, "Radiative tau decay and the magnetic moment of the muon", JHEP 0208, 002 (2002). e-Print: hep-ph/0207310 [hep-ph]
- A. Miranda and P. Roig. "New τ -based evaluation of the hadronic contribution to the vacuum polarization piece of the muon anomalous magnetic moment". Phys.Rev.D 102 (2020) 114017. e-Print: 2007.11019 [hep-ph]
- G. Colangelo et al. "Data-driven evaluations of Euclidean windows to scrutinize hadronic vacuum polarization". Published in: Phys.Lett.B 833 (2022) 137313. e-Print: 2205.12963 [hep-ph]
- P. Masjuan, A. Miranda and P. Roig. "τ data-driven evaluation of Euclidean windows for the hadronic vacuum polarization". Published in: Phys.Lett.B 850 (2024) 138492. e-Print: 2305.20005 [hep-ph]
- M. Davier, A. Hoecker, A.M. Lutz, B. Malaescu, Z. Zhang. "Tensions in $e^+e^-\to\pi^+\pi^-(\gamma)$ measurements: the new landscape of data-driven hadronic vacuum polarization predictions for the muon g-2". e-Print: 2312.02053 [hep-ph]

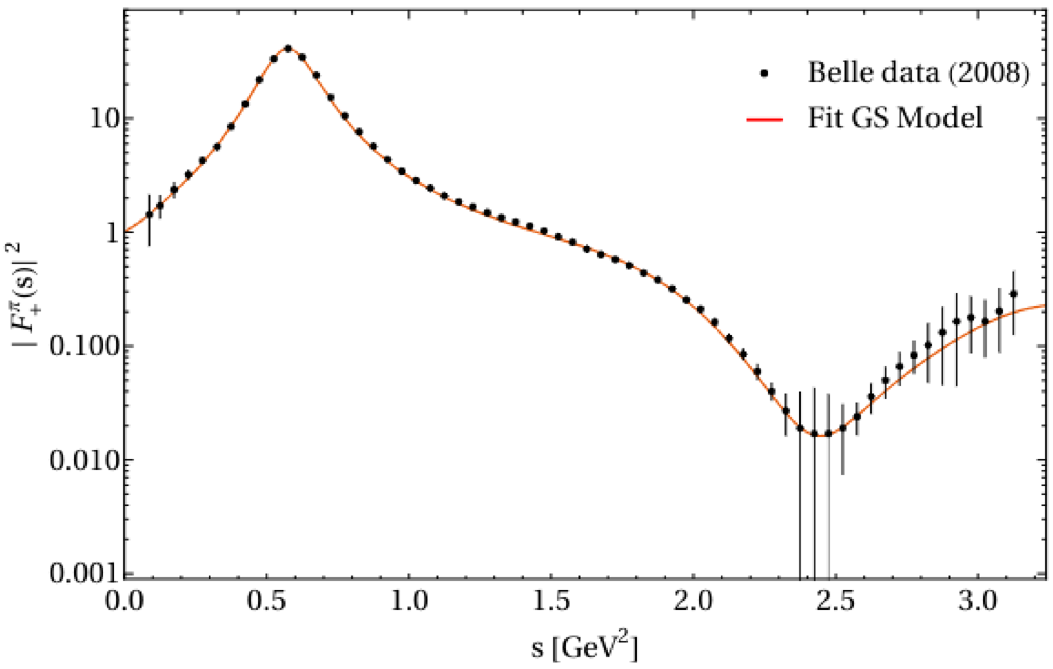
Belle data (2008)
Fit GS Model
$|F_+^\pi(s)|^2$
s [GeV$^2$]

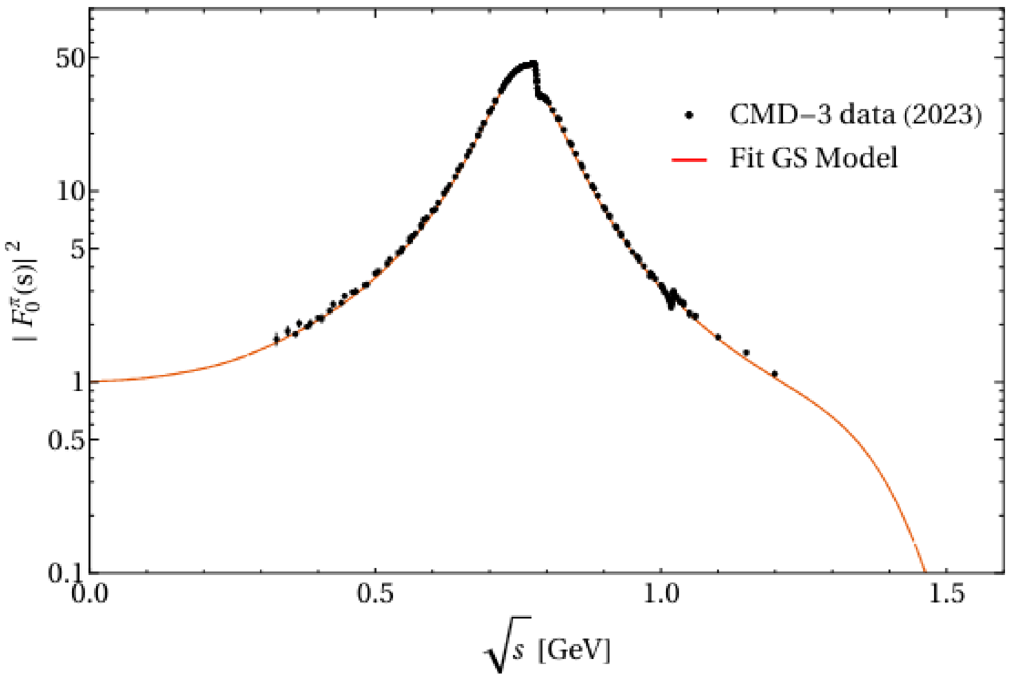
CMD−3 data (2023)
Fit GS Model
$|F_0^\pi(s)|^2$
$\sqrt{s}$ [GeV]

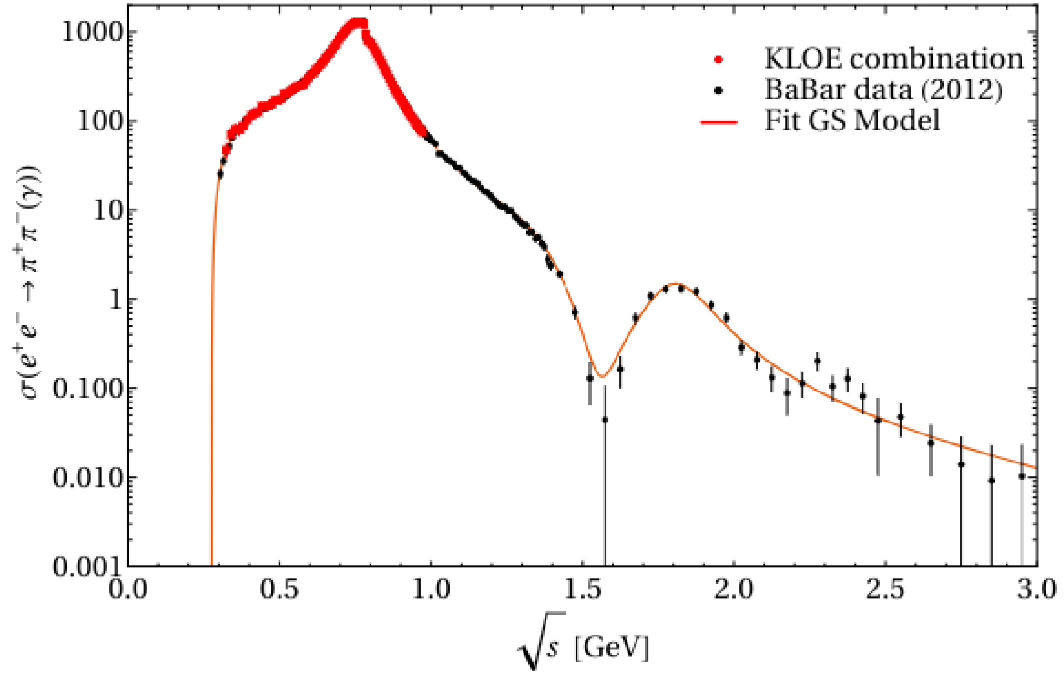
KLOE combination
BaBar data (2012)
Fit GS Model
$\sigma(e^+e^- \to \pi^+\pi^-(\gamma))$
$\sqrt{s}$ [GeV]

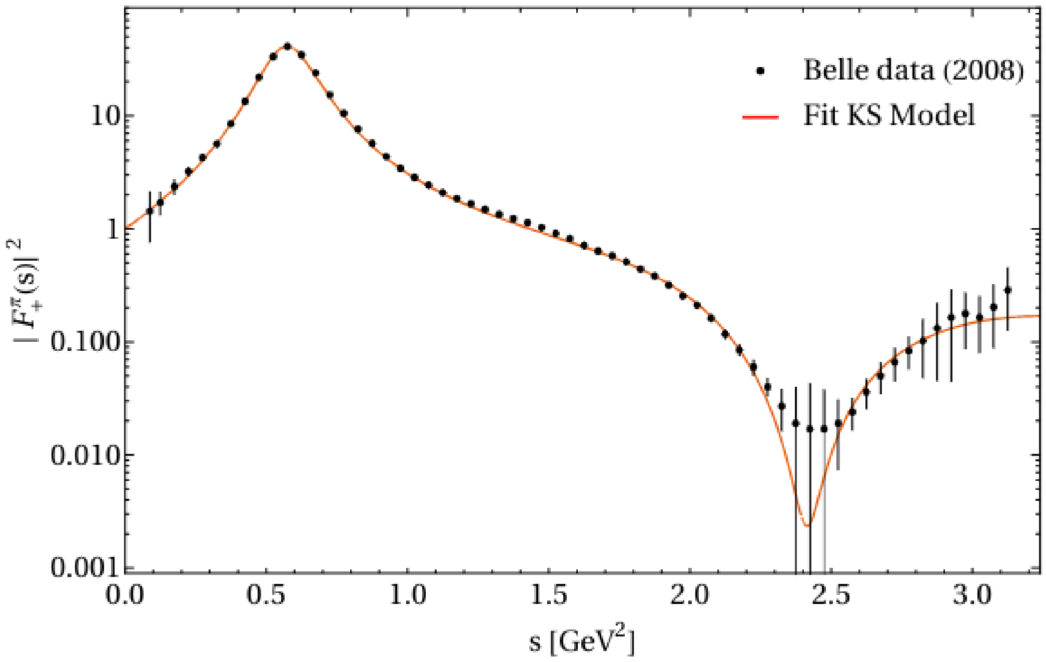
Belle data (2008)
Fit KS Model
$|F_+^\pi(s)|^2$
s [GeV$^2$]

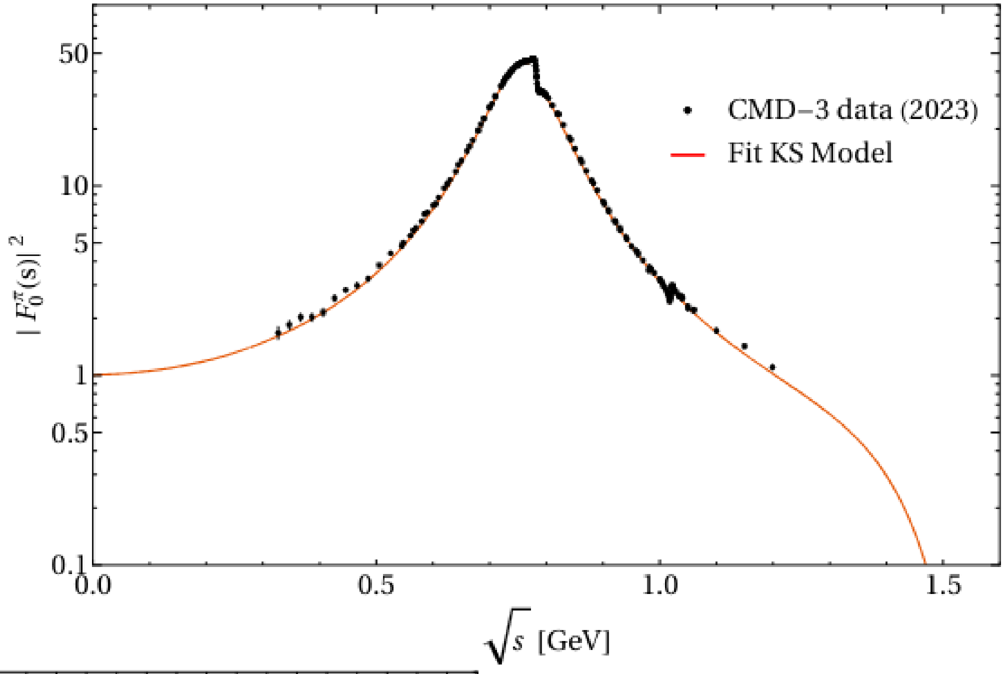
CMD−3 data (2023)
Fit KS Model
$|F_0^\pi(s)|^2$
$\sqrt{s}$ [GeV]

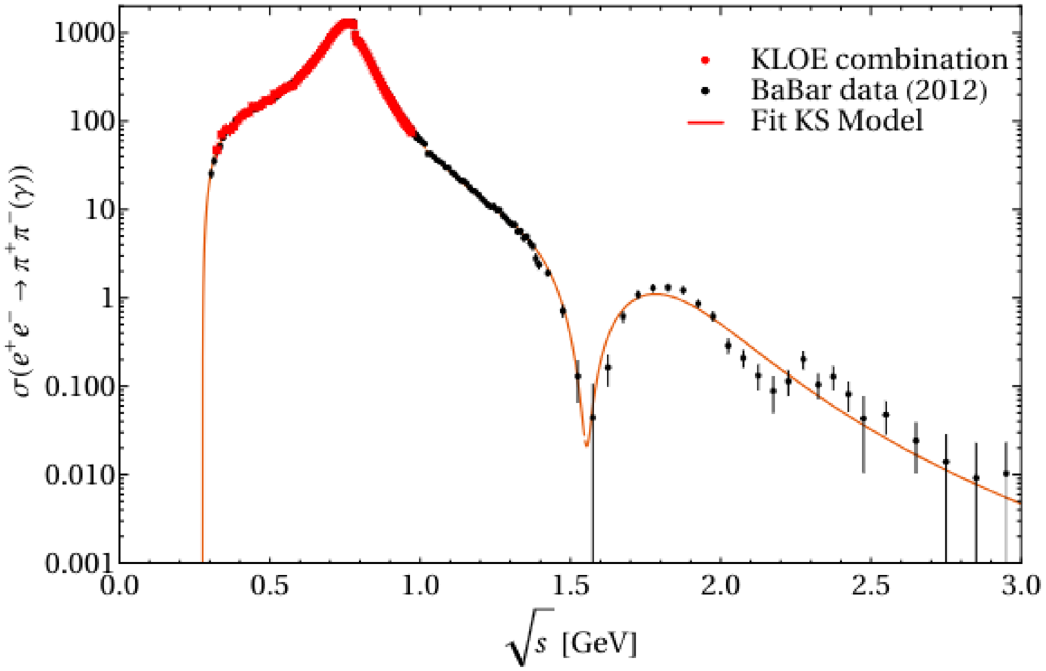
KLOE combination
BaBar data (2012)
Fit KS Model
$\sigma(e^+e^- \to \pi^+\pi^-(\gamma))$
$\sqrt{s}$ [GeV]

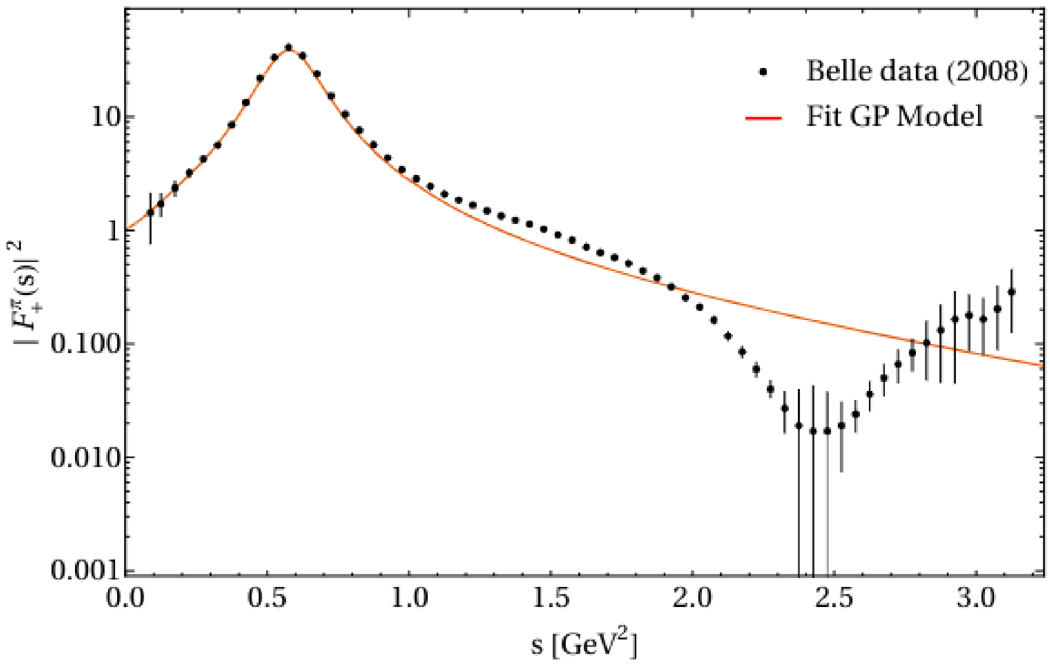

Belle data (2008)
Fit GP Model
$|F_+^\pi(s)|^2$
s [GeV$^2$]
10
1
0.100
0.010
0.001
0.0
0.5
1.0
1.5
2.0
2.5
3.0


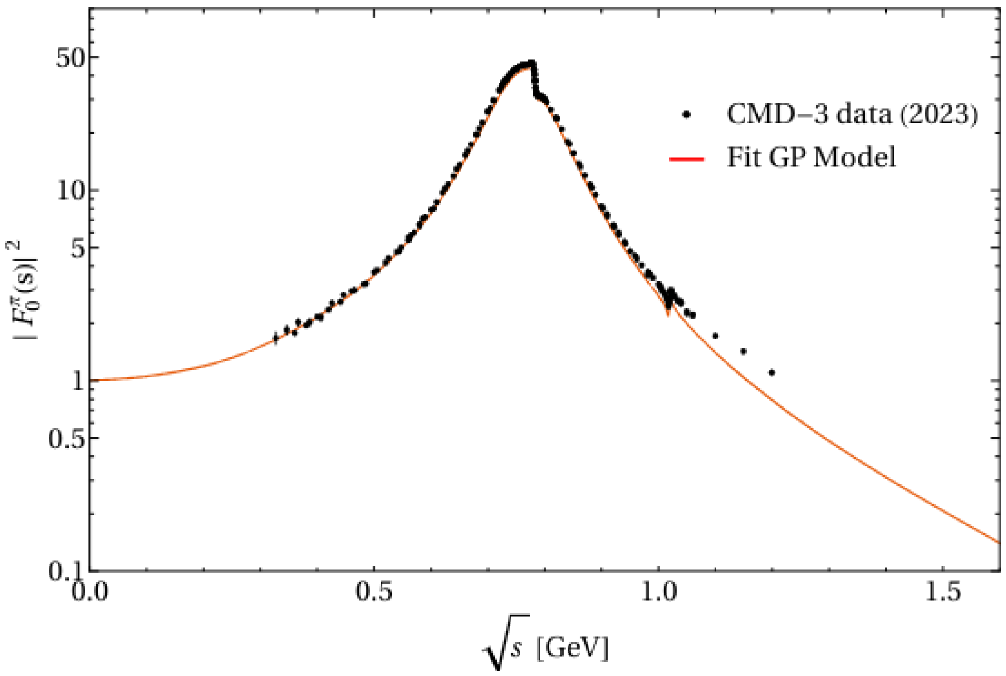

CMD−3 data (2023)
Fit GP Model
$|F_0^\pi(s)|^2$
$\sqrt{s}$ [GeV]
50
10
5
1
0.5
0.1
0.0
0.5
1.0
1.5


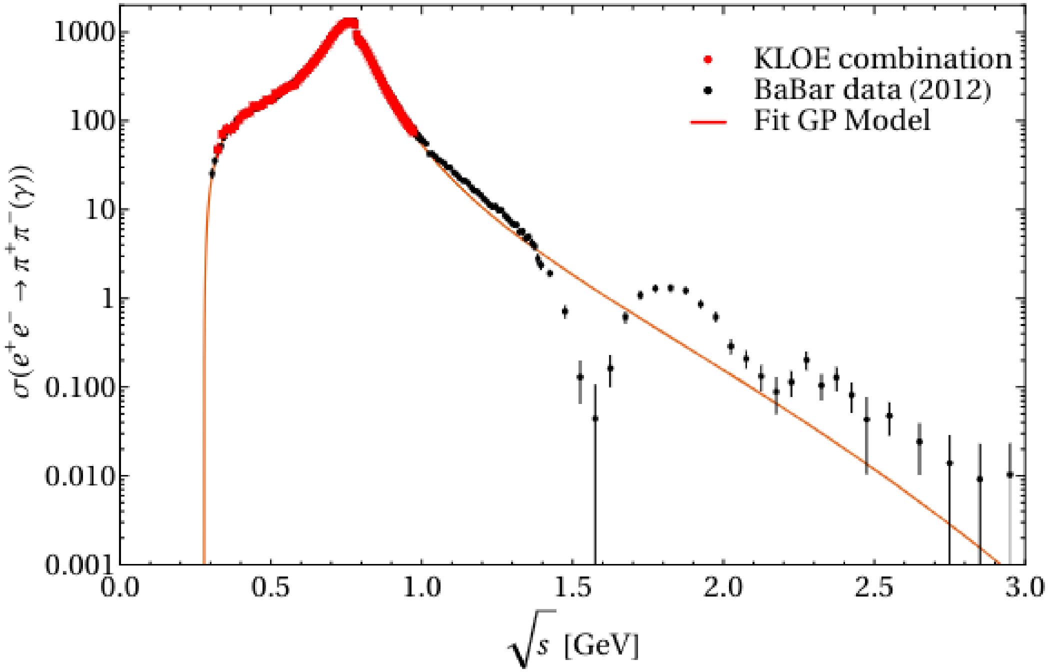

KLOE combination
BaBar data (2012)
Fit GP Model
$\sigma(e^+e^- \to \pi^+\pi^-(\gamma))$
$\sqrt{s}$ [GeV]
1000
100
10
1
0.100
0.010
0.001
0.0
0.5
1.0
1.5
2.0
2.5
3.0

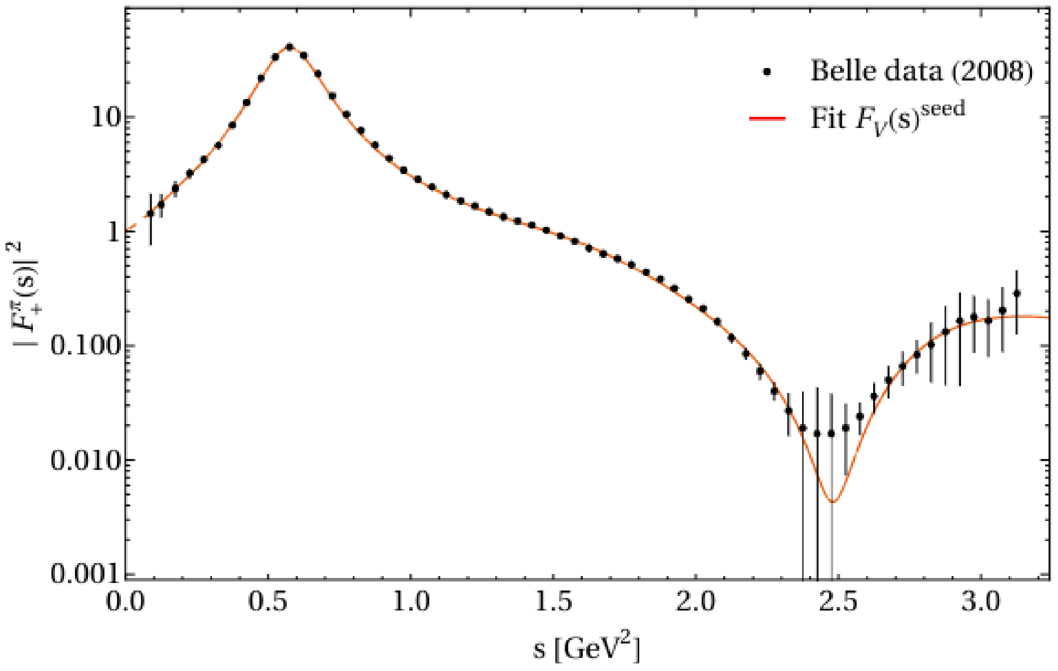

Belle data (2008)
Fit $F_V(s)^{seed}$
$|F_+^\pi(s)|^2$
s [GeV$^2$]


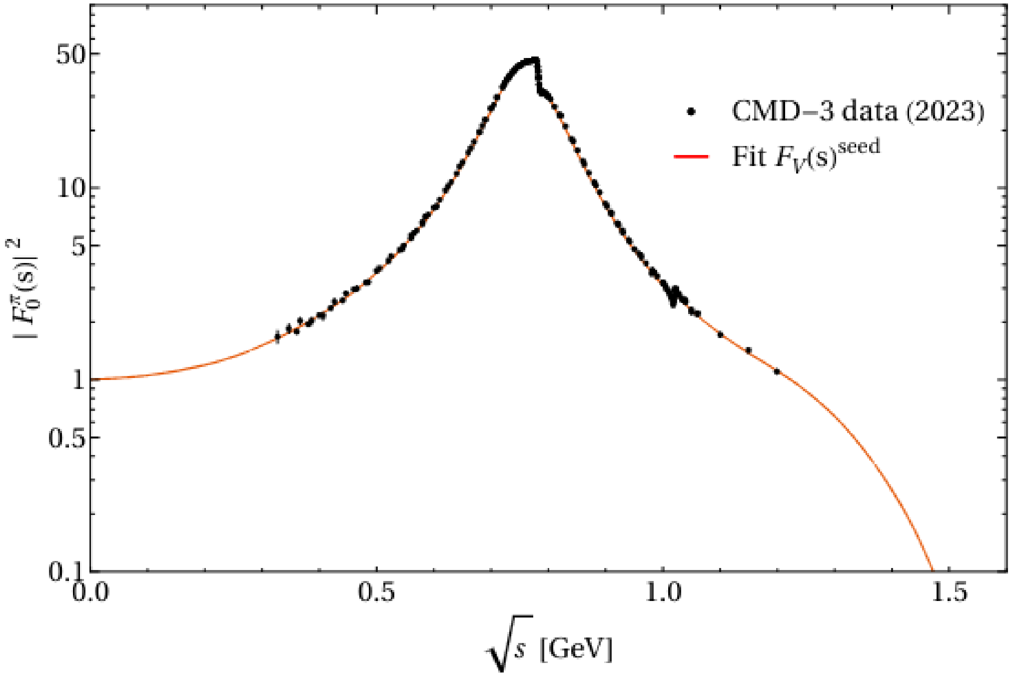

CMD−3 data (2023)
Fit $F_V(s)^{seed}$
$|F_0^\pi(s)|^2$
$\sqrt{s}$ [GeV]


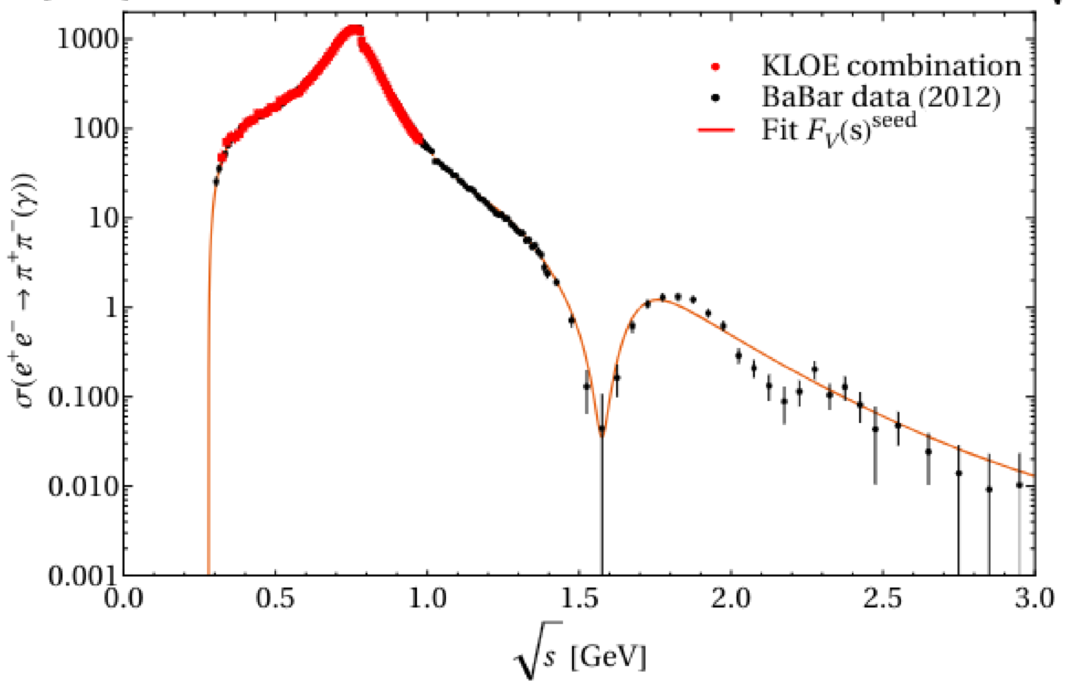

KLOE combination
BaBar data (2012)
Fit $F_V(s)^{seed}$
$\sigma(e^+e^- \to \pi^+\pi^-(\gamma))$
$\sqrt{s}$ [GeV]

# Isospin-breaking corrections

| Source | $\Delta\mathcal{B}^{\text{CVC}}_{\pi^-\pi^0}$ ($10^{-2}$) GS model | KS model |
|---|---|---|
| $S_{\text{EW}}$ | $+0.57 \pm 0.01$ | |
| $G_{\text{EM}}$ | $-0.07 \pm 0.17$ | |
| FSR | $-0.19 \pm 0.02$ | |
| $\rho$–$\omega$ interference | $-0.01 \pm 0.01$ | $-0.02 \pm 0.01$ |
| $m_{\pi^\pm} - m_{\pi^0}$ effect on $\sigma$ | $+0.19$ | |
| $m_{\pi^\pm} - m_{\pi^0}$ effect on $\Gamma_\rho$ | $-0.22$ | |
| $m_{\rho^\pm} - m_{\rho^0_{\text{bare}}}$ | $+0.08 \pm 0.08$ | $+0.09 \pm 0.08$ |
| $\pi\pi\gamma$, electrom. decays | $+0.34 \pm 0.03$ | $+0.37 \pm 0.04$ |
| Total | $+0.69 \pm 0.19$ | $+0.72 \pm 0.19$ |
| | $+0.69 \pm 0.22$ | |

Eur. Phys. J. C66, 127 (2010)